American Journal of Pathology, Vol. 165, No. 2, August 2004

The 14-3-3 Protein ε Isoform Expressed in Reactive Astrocytes in Demyelinating Lesions of Multiple Sclerosis Binds to Vimentin and Glial Fibrillary Acidic Protein in Cultured Human Astrocytes

Jun-ichi Satoh,* Takashi Yamamura,* and Kunimasa Arima†

From the Department of Immunology, National Institute of Neuroscience, and the Department of Neuropathology,† National Center Hospital for Mental, Nervous, and Muscular Disorders, National Center of Neurology and Psychiatry, Tokyo, Japan*

The 14-3-3 protein family consists of acidic 30-kd proteins expressed at high levels in neurons of the central nervous system. Seven isoforms form a dimeric complex that acts as a molecular chaperone that interacts with key signaling components. Recent studies indicated that the 14-3-3 protein identified in the cerebrospinal fluid of various neurological diseases including multiple sclerosis (MS) is a marker for extensive brain destruction. However, it remains unknown whether the 14-3-3 protein plays an active role in the pathological process of MS. To investigate the differential expression of seven 14-3-3 isoforms in MS lesions, brain tissues of four progressive cases were immunolabeled with a panel of isoform-specific antibodies. Reactive astrocytes in chronic demyelinating lesions intensely expressed β, ε, ζ, η, and σ isoforms, among which the ε isoform is a highly specific marker for reactive astrocytes. Furthermore, protein overlay, mass spectrometry, immunoprecipitation, and double-immunolabeling analysis showed that the 14-3-3 protein interacts with both vimentin and glial fibrillary acidic protein in cultured human astrocytes. These results suggest that the 14-3-3 protein plays an organizing role in the intermediate filament network in reactive astrocytes at the site of demyelinating lesions in MS. ***(Am J Pathol 2004, 165:577–592)***

The 14-3-3 protein family consists of evolutionarily conserved, acidic 30-kd proteins originally identified by two dimensional analysis of brain protein extract.[1–4] Seven isoforms of the 14-3-3 protein named β, γ, ε, ζ, η, θ (also termed as τ), and σ have been identified in eukaryotic cells. Although the 14-3-3 protein is widely distributed in neural and nonneural tissues, it is expressed most abundantly in neurons in the central nervous system (CNS), where it represents 1% of total cytosolic proteins.[4–7] A homodimeric or heterodimeric complex, which is composed of the same or distinct isoforms of the 14-3-3 protein, constitutes a large cup-like structure with two ligand-binding sites in its groove. The dimeric complex acts as a novel molecular chaperone that interacts with key molecules involved in cell differentiation, proliferation, transformation, and apoptosis.[1–4] It regulates the function of target proteins by restricting their subcellular location, bridging them to modulate catalytic activity, and protecting them from dephosphorylation or proteolysis.[1–4,8–10] In general, the 14-3-3 protein binds to phosphoserine-containing motifs of the ligands such as RSXpSXP and RXY/FXpSXP in a sequence-specific manner.[1–3,10] More than 100 proteins have been identified as being 14-3-3 binding partners, including a range of intracellular signaling regulators such as Raf, BAD, protein kinase C (PKC), phophatidylinositol 3-kinase (PI3K), and cdc25 phosphatase.[1–4,8–10] Binding of the 14-3-3 protein to Raf is indispensable for Raf kinase activity in the Ras/MAPK signaling pathway, whereas 14-3-3 binding to the mitochondrial Bcl-2 family member BAD, when phosphorylated by a serine/threonine kinase Akt, inhibits apoptosis.[1–4] In addition to the phosphorylation-dependent interaction, the 14-3-3 protein can interact with a set of target proteins in a phosphorylation-independent manner.[10–12] The ε isoform binds to p190RhoGEF via a phosphoserine-independent interaction.[11]

Previous studies indicated that the 14-3-3 protein has isoform-specific and nonredundant functions.[1–4] Synaptic transmission and associative learning are impaired in

Supported by the Grant-in-Aid for Scientific Research (B2-15390280 and PA007-16017320); the Ministry of Education, Science, Sports, and Culture; and the Organization for Pharmaceutical Safety and Research, Kiko, Japan.

Accepted for publication April 22, 2004.

During submission of the present manuscript, an immunohistochemical study (Kawamoto Y, Akiguchi I, Kovács GG, Flicker H, Budka H: Increased 14-3-3 immunoreactivity in glial elements in patients with multiple sclerosis. Acta Neuropathol 2004, 107:137–143) has been published. This study showed that the 14-3-3 protein is expressed strongly in both astrocytes and oligodendrocytes in MS brains using an anti-14-3-3 protein antibody broadly reactive against all isoforms (H-8, sc-1657; Santa Cruz Biotechnology).

Supplemental information can be found on *http://www.amjpathol.org*.

Address reprint requests to Dr. Jun-ichi Satoh, Department of Immunology, National Institute of Neuroscience, NCNP, 4-1-1 Ogawahigashi, Kodaira, Tokyo 187-8502, Japan. E-mail: satoj@ncnp.go.jp.

Drosophila mutants lacking the ζ protein.[13] The 14-3-3 isoforms have distinct affinities for their target proteins. A preferential interaction is observed between PKCθ and the human 14-3-3θ isoform in T cells,[14] IGF1-receptor, IRS1, and ε isoform,[15] the apoptosis-inhibitor A20 and the human β and η isoforms,[16] and glucocorticoid receptor and the human η isoform.[17] The human β and ζ isoforms and not γ or ε isoforms interact with phosphorylated tau.[18] Furthermore, different isoforms show distinct patterns of spatial, temporal, and subcellular distribution. The human θ and σ isoforms are predominantly expressed in T cells and epithelial cells, respectively.[14,19] The rat ε and γ isoforms are enriched in the synaptosomal membranes,[20] and the γ isoform is the main 14-3-3 protein located in the Golgi apparatus in mammalian cells.[3] In the developing rat brain, defined populations of neurons express β, γ, ζ, and θ isoforms at specific stages of development.[6,7] In the adult mouse brain, β, γ, η, and ζ isoforms are widely distributed with the localization primarily in neurons, although some glial cells express ε, θ, and ζ isoforms.[21]

Recently, several lines of evidence have indicated that the 14-3-3 protein is involved in neurodegenerative processes. The 14-3-3 protein detected in the cerebrospinal fluid of Creutzfeldt-Jacob disease has been used as a biochemical marker for the premortem diagnosis of Creutzfeldt-Jacob disease in the context of differential diagnosis of progressive dementia.[22–24] In addition, intense immunoreactivity against the ζ isoform was identified in amyloid plaques in the Creutzfeldt-Jacob disease brain.[25] However, several studies including our own showed that the 14-3-3 protein is occasionally detectable in the cerebrospinal fluid of infectious meningoencephalitis, metabolic encephalopathy, cerebrovascular diseases, and multiple sclerosis (MS) presenting with severe myelitis, suggesting that it is not a marker specific for prion diseases but for extensive destruction of brain tissues causing the leakage of 14-3-3 protein into the cerebrospinal fluid.[4,22,26,27] In the Alzheimer's disease brain, neurofibrillary tangles express immunoreactivity against the 14-3-3 protein.[28] The 14-3-3ζ homodimer interacts with tau and glycogen synthase kinase-3β (GSK3β), and stimulates GSK3β-mediated tau phosphorylation.[29] In the Parkinson's disease brain, Lewy bodies possess γ, ε, ζ, and θ isoforms that interact with α-synuclein.[30,31] Dopamine-dependent neurotoxicity is mediated by a soluble complex composed of the 14-3-3 protein and α-synuclein, whose levels are markedly elevated in the substantia nigra of the Parkinson's disease brain.[32] The neurotoxicity of ataxin-1, the causative protein of spinocerebellar ataxia type 1, is enhanced by ε and ζ isoforms that bind to and stabilize ataxin-1 phosphorylated by Akt, thereby slowing its degradation.[33] Finally, expression of the θ isoform is enhanced in the spinal cord of amyotrophic lateral sclerosis.[34] However, it remains unknown whether the 14-3-3 protein plays an active role in the pathological process of MS.

In the present study, we investigated the differential expression of seven 14-3-3 isoforms in chronic active demyelinating lesions of MS. We found that reactive astrocytes intensely express β, ε, ζ, η, and σ isoforms, among which the ε isoform provides a specific marker to identify reactive astrocytes in the MS brain. Furthermore, the 14-3-3 protein interacts with vimentin and glial fibrillary acidic protein (GFAP) in cultured human astrocytes. These observations suggest that the 14-3-3 protein plays an organizing role in the intermediate filament (IF) network in reactive astrocytes at the site of demyelinating lesions in MS.

Materials and Methods

MS and Non-MS Brain Tissues

Ten-μ-thick tissue sections were prepared from the brain, spinal cord, and optic nerve derived from four autopsy cases of MS numbered 791, 744, 609, and 544. The clinical and neuroradiological profiles of these patients are shown in a supplementary table on The American

Table 1. The14-3-3 Isoform-Specific or Broadly Reactive Antibodies Utilized for Immunochemistry and Western Blot Analysis

14-3-3 isoforms	Suppliers	Code	Antigen peptide	Origin	Specificity	Concentration used for immunohistiochemistry (μg/ml)	Concentration used for Western blotting (μg/ml)
Pan	SC	sc-629	N-terminal	Rabbit	Reactive to all isoforms	0.4	0.04
Pan	SC	sc-1657	N-terminal	Mouse	Reactive to all isoforms	0.4	0.04
β	SC	sc-628	C-terminal	Rabbit	Reactive predominantly to β isoform, but crossreactive to other isoforms to a lesser extent	0.4	0.04
β	IBL	18641	N-terminal	Rabbit	Not crossreactive to other isoforms	2	1
γ	IBL	18647	C-terminal	Rabbit	Not crossreactive to other isoforms	5	0.2
ε	IBL	18643	C-terminal	Rabbit	Not crossreactive to other isoforms	2	1
ζ	IBL	18644	N-terminal	Rabbit	Not crossreactive to other isoforms	2	0.5
η	IBL	18645	N-terminal	Rabbit	Not crossreactive to other isoforms	5	1
θ (τ)	SC	sc-732	C-terminal	Rabbit	Not crossreactive to other isoforms	0.4	0.04
θ (τ)	IBL	10017	Recombinant, whole	Mouse	Minimally crossreactive to σ isoform	1	1
σ	IBL	18642	C-terminal	Rabbit	Not crossreactive to other isoforms	1	1

Abbreviations: SC, Santa Cruz Biotechnology; IBL, Immunobiological Laboratory. The specificity of the antibodies (IBL) is also shown on Supplementary Figure 1 at *http://www.amjpathol.org.*

Journal of Pathology website (*http://www.amjpathol.org*). The tissues were fixed with 4% paraformaldehyde (PFA) or 10% neutral formalin and embedded in paraffin. For the controls, tissue sections were prepared from the autopsied brains of six non-MS neurological and psychiatric disease cases that include a 47-year-old man with acute cerebral infarction who died of sepsis (no. 719), an 84-year-old man with acute cerebral infarction who died of disseminated intravascular coagulation (no. 786), a 62-year-old man with old cerebral infarction who died of pancreatic cancer (no. 789), a 56-year-old man with old cerebral infarction who died of myocardial infarction (no. 807), a 36-year-old woman with schizophrenia who died of lung tuberculosis (no. 523), and a 61-year-old man with schizophrenia who died of asphyxia (no. 826). In addition, they were prepared from the autopsied brains of six neurologically normal patients that include a 79-year-old woman who died of hepatic cancer (no. G6), a 75-year-old woman who died of breast cancer (no. G7), a 60-year-old woman who died of external auditory canal cancer (no. G8), a 74-year-old woman who died of gastric and hepatic cancers (no. G9), an 83-year-old woman who died of gastric cancer and myocardial infarction (no. A2623), and a 65-year-old man who died of liver cirrhosis and bronchopneumonia (no. A2647). Autopsies on all patients were performed at the National Center Hospital for Mental, Nervous, and Muscular Disorders, NCNP, Tokyo, Japan. Written informed consent was obtained in all cases.

Immunohistochemistry and Immunocytochemistry

After deparaffination, the tissue sections were heated by microwave at 95°C for 10 minutes in 10 mmol/L citrate sodium buffer (pH 6.0). They were then treated at room temperature for 15 minutes with 3% H_2O_2-containing methanol. For vimentin immunolabeling, the tissue sections were pretreated with 0.125% trypsin solution (Nichirei, Tokyo, Japan) at 37°C for 15 minutes. They were then incubated with 10% normal goat serum containing phosphate-buffered saline (PBS) at room temperature for 15 minutes to block nonspecific staining. The sections were incubated in a moist chamber at 4°C overnight with a panel of 14-3-3 isoform-specific antibodies or with antibodies broadly reactive against all isoforms listed in Table 1. The antibodies were obtained from Immunobiological Laboratory (IBL), Gumma, Japan, and Santa Cruz Biotechnology, Santa Cruz, CA. The specificity of the antibodies from IBL is shown in Supplementary Figure 1 on The American Journal of Pathology website, and additional information on those of Santa Cruz Biotechnology is available on the supplier's website (*www.scbt.com*). After washing with PBS, the tissue sections were labeled at room temperature for 30 minutes with peroxidase-conjugated secondary antibodies (Simple Stain MAX-PO kit, Nichirei) followed by incubation with a colorizing solution containing diaminobenzidine tetrahydrochloride and a counterstain with hematoxylin. To identify cell types expressing the 14-3-3 protein, adjacent sections were stained with the following antibodies: rabbit polyclonal antibody against GFAP (N1506; DAKO, Carpinteria, CA), rabbit polyclonal antibody against vimentin (H-84; Santa Cruz Biotechnology), mouse monoclonal antibody against vimentin (V9; Santa Cruz Biotechnology), rabbit polyclonal antibody against myelin basic protein (N1546; DAKO), mouse monoclonal antibody against CD68 (N1577; DAKO), and mouse monoclonal antibody against 70-kd and 200-kd neurofilament proteins (2F11; Nichirei). For negative controls, sections were incubated with a rabbit-negative control reagent (DAKO) instead of primary antibodies. The optimum concentrations of these antibodies and incubation periods were determined according to the supplier's instruction.

For double-labeling immunocytochemistry, cells on cover glasses were fixed with 4% PFA in 0.1 mol/L phos-

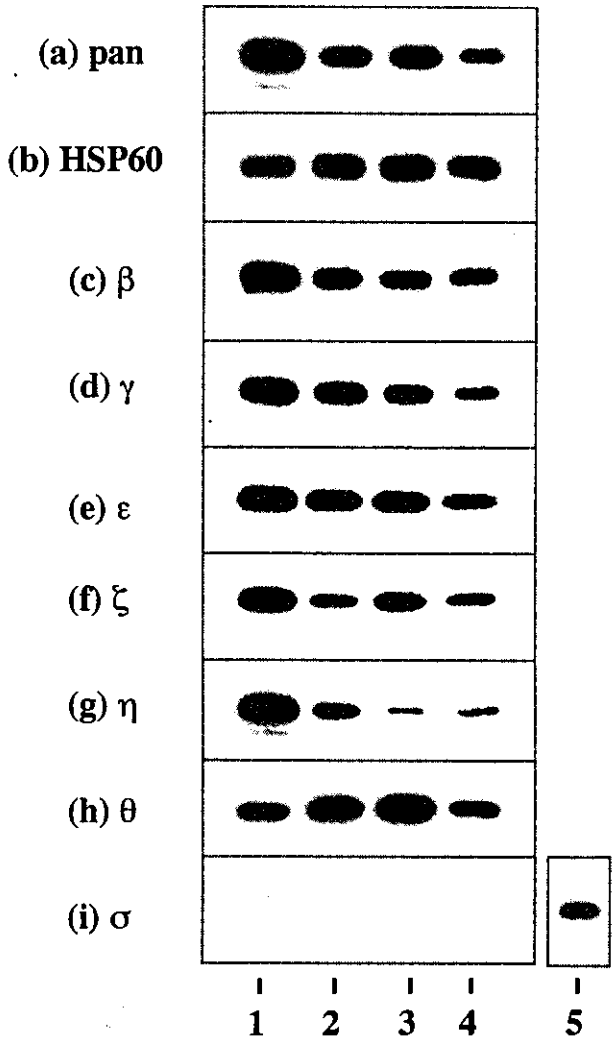

Figure 1. Constitutive expression of 14-3-3 isoforms in cultured human cells. Two μg of total protein extract isolated from brain tissues or cultured cells incubated in 10% FBS-containing medium were processed for Western blot analysis using a battery of 14-3-3 isoform-specific antibodies or the antibodies broadly reactive against all of the isoforms listed in Table 1, or the antibody against the housekeeping gene product HSP60. **a** to **i** indicate the following antibody specificity: **a**, all isoforms; **b**, HSP60; **c**, β; **d**, γ; **e**, ε; **f**, ζ; **g**, η; **h**, θ; and **i**, σ. **Lanes 1** to **4** represent homogenate of the human cerebrum (**lane 1**), NTera2-derived differentiated neurons (NTera2-N) (**lane 2**), U-373MG astrocytoma cells (**lane 3**), fetal human astrocytes (AS1477) (**lane 4**), and HeLa cervical carcinoma cells (**lane 5**).

phate buffer (pH 7.4) at room temperature for 10 minutes, followed by incubation with PBS containing 0.5% Triton X-100 at room temperature for 20 minutes.[26] The cells were then incubated at room temperature for 30 minutes with a mixture of 14-3-3 isoform-specific antibody and rat monoclonal anti-GFAP antibody (2.2B10) or V9 antibody. Next, they were incubated at room temperature for 30 minutes with a mixture of rhodamine-conjugated anti-rabbit IgG and fluorescein isothiocyanate-conjugated anti-rat or mouse IgG (ICN-Cappel, Aurora, OH). After several washes, cover glasses were mounted on the slides with glycerol-polyvinyl alcohol, and the slides were examined under a Nikon ECLIPSE E800 universal microscope equipped with fluorescein and rhodamine optics. Negative controls were processed following these steps except for exposure to primary antibody.

Cell Culture

Two different sources of cultured human astrocytes were used. One was fetal human astrocytes named AS1477, provided by Drs. K. Watabe and S. U. Kim of the University of British Columbia, Vancouver, BC, Canada. They were maintained in Dulbecco's modified Eagle's medium (DMEM) supplemented with 10% fetal bovine serum (FBS), 100 U/ml penicillin, and 100 μg/ml streptomycin (feeding medium). The other was astrocytes named AS-BW, whose differentiation was induced from neuronal progenitor (NP) cells. NP cells isolated from the brain of a human fetus at 18.5 weeks of gestation were obtained from BioWhittaker (Walkersville, MD). NP cells plated on a polyethyleneimine-coated surface were incubated in DMEM/F-12 medium containing an insulin-transferrin-selenium supplement (Invitrogen, Carlsbad, CA), 20 ng/ml recombinant human epidermal growth factor (Higeta, Tokyo, Japan), 20 ng/ml recombinant human basic fibroblast growth factor (PeproTech EC, London, UK), and 10 ng/ml recombinant human leukemia inhibitory factor (Chemicon, Temecula, CA) (NP medium).[35] For the induction of astrocyte differentiation, NP cells were incubated for several weeks in feeding medium instead of NP medium. This incubation induced vigorous proliferation and differentiation of astrocytes accompanied by a rapid reduction in nonastroglial cell types. Newborn mouse astrocytes were prepared as previously described.[26] In some experiments, cultured human and mouse astrocytes were plated at subconfluent density and incubated for 7 days in serum-free DMEM/F-12 medium supplemented with insulin-transferrin-selenium without inclusion of any other growth factors or in 10% FBS-containing DMEM/F-12 medium supplemented with insulin-transferrin-selenium.

Human cell lines such as U-373MG astrocytoma, NTera2 teratocarcinoma and HeLa cervical carcinoma were obtained from the RIKEN Cell Bank (Tsukuba, Japan) and the American Type Culture Collection (Rockville, MD). For the induction of neuronal differentiation, NTera2 cells maintained in the undifferentiated state (NTera2-U) were incubated for 4 weeks in feeding me-

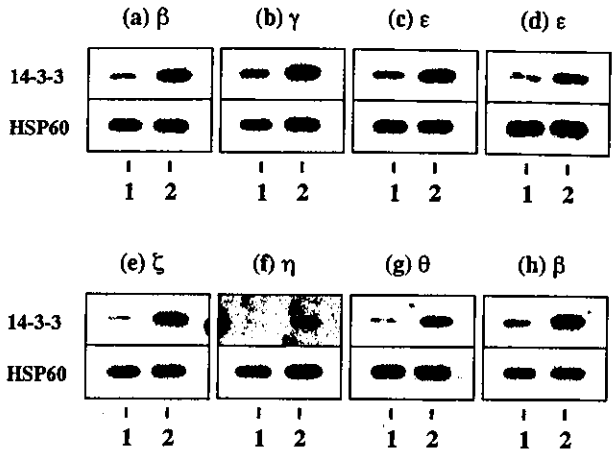

Figure 2. Growth-dependent expression of various 14-3-3 isoforms in cultured human astrocytes. Human and mouse astrocytes were plated at subconfluent density and incubated for 7 days in the serum-free culture medium or in 10% FBS-containing culture medium. Two μg of total protein extract was processed for Western blot analysis using a battery of 14-3-3 isoform-specific antibodies or with the antibodies broadly reactive against all isoforms (**top**). After stripping the antibodies, identical blots were relabeled with the antibody against HSP60 for the standardization of expression levels (**bottom**). **a** to **g** (**top**) indicate the expression of β (**a**), γ (**b**), ε (**c**), ζ (**e**), η (**f**), and θ (**g**) in human astrocytes (AS1477); ε in human astrocytes (AS-BW) (**d**); and β in mouse astrocytes (**h**). **Lanes 1** and **2** represent the cells cultured under the serum-free growth-arrested condition (**lane 1**) or the serum-containing growth-promoting condition (**lane 2**). Additional data are shown in supplementary Figure 2 on the American Journal of Pathology website.

Table 2. Differential Expression of Seven 14-3-3 Isoforms in Glial Cells and Neurons in MS and Control Brains

Brains 14-3-3 isoforms/cell types	Astrocytes			Microglia/macrophages			Oligodendrocytes			Neurons		
	MS	OND	NNC	MS	OND	NNC	MS	OND	NNC	MS	OND	NNC
β	maj (++)	maj (+)	no (−)	maj (++)	maj (++)	no (−)	min (+)	no (−)	no (−)	maj (++)	maj (++)	maj (++)
γ	min (++)	min (+)	no (−)	min (++)	min (+)	no (−)	no (−)	no (−)	no (−)	maj (++)	maj (++)	maj (++)
ε	maj (++)	maj (++)	min (+)	no (−)	no (−)	no (−)	no (−)	no (−)	no (−)	min (+)	min (+)	min (+)
ζ	maj (++)	maj (++)	no (−)	maj (++)	maj (++)	no (−)	no (−)	no (−)	no (−)	maj (++)	maj (++)	maj (++)
η	maj (++)	maj (++)	no (−)	maj (++)	min (++)	no (−)	no (−)	no (−)	no (−)	maj (++)	maj (++)	maj (++)
θ	min (+)	min (+)	no (−)	no (−)	no (−)	no (−)	min (++)	min (++)	min (+)	min (+)	min (+)	min (+)
σ	min (++)	min (++)	min (+)	no (−)	no (−)	no (−)	no (−)	no (−)	no (−)	no (−)	no (−)	no (−)

The present study includes four MS cases numbered #791, 744, 609, and 544 whose clinical profiles are given in a supplementary table on the AJP website, six non-MS neurological and psychiatric disease cases (OND) composed of #719 acute cerebral infarction, #786 acute cerebral infarction, #789 old cerebral infarction, #807 old cerebral infarction, #523 schizophrenia, and #826 schizophrenia, and six neurologically normal cases (NNC) composed of #G6, #G7, #G8, #G9, #A2623, and #A2647, whose profiles are described in the Materials and Methods section.

The population size of the immunoreactive cells is expressed as maj, major (large) population; min, minor (small) population; and no, almost no population. The intensity of immunoreactivity is graded as (−) negative, (+) weak, and (++) intense.

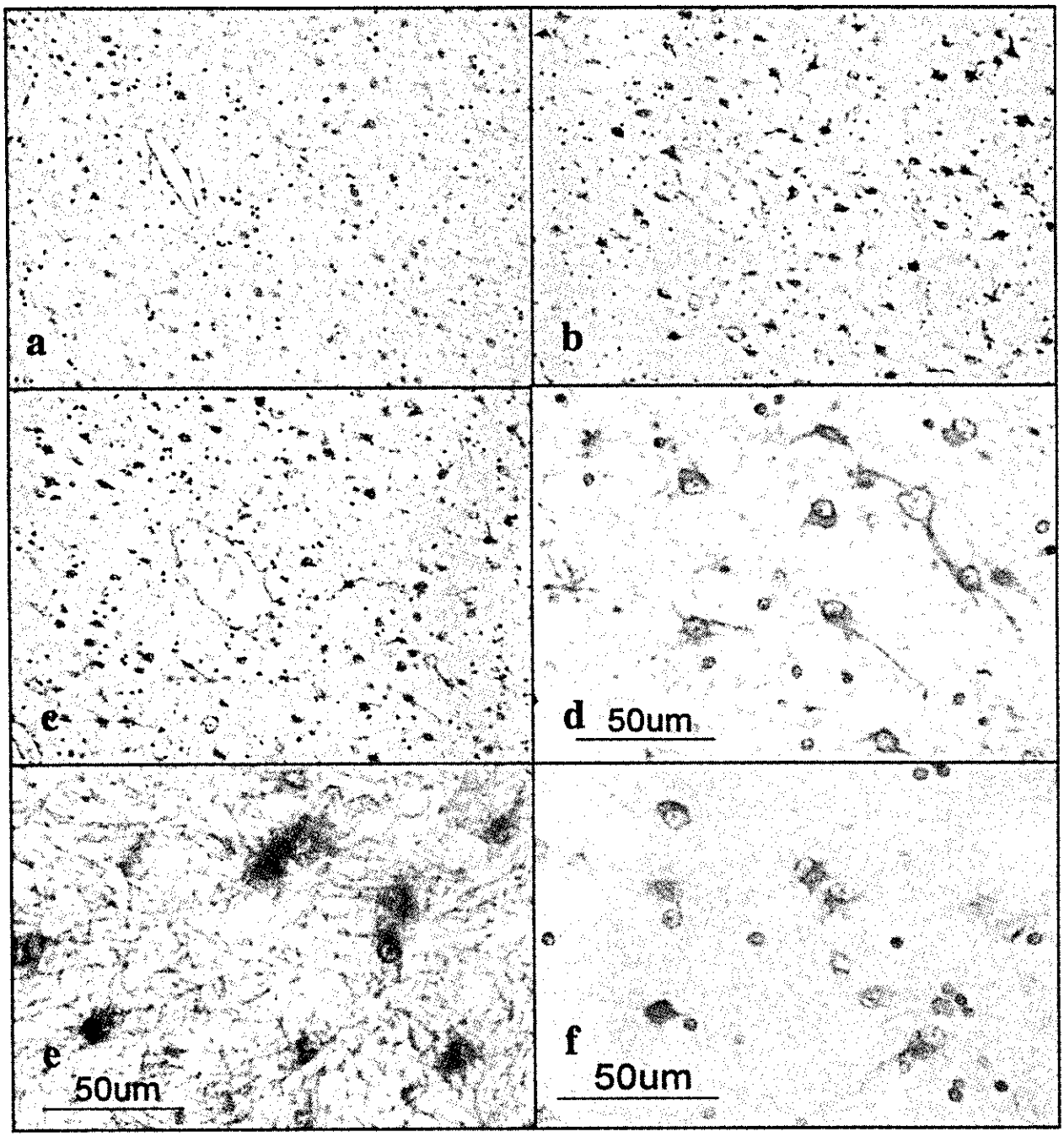

Figure 3. The 14-3-3 ε isoform is expressed in reactive astrocytes in chronic demyelinating lesions of MS. MS brain tissues were processed for immunohistochemical analysis using ε isoform-specific antibody or the antibody against GFAP or vimentin. **a** to **f** represent the following: **a:** no. 744 MS, chronic active demyelinating lesions in the subcortical white matter of the frontal lobe (H&E). **b:** No. 744 MS, the area corresponding to **a** (GFAP). Many reactive astrocytes are stained. **c:** No. 744 MS, the area corresponding to **a** (ε). Many reactive astrocytes are stained. **d:** No. 744 MS, a higher magnification view of **c** (ε). Reactive astrocytes are stained. **e:** No. 544 MS, chronic inactive demyelinating lesions in the optic nerve (ε). Reactive astrocytes and the glial scar are stained. **f:** No. 744 MS, chronic active demyelinating lesions in the subcortical white matter of the frontal lobe (vimentin). Reactive astrocytes are stained.

dium containing 10^{-5} mol/L *all trans* retinoic acid (Sigma, St. Louis, MO), replated twice and then plated on a surface coated with Matrigel Basement Membrane Matrix (Becton Dickinson, Bedford, MA). They were incubated for another 2 weeks in feeding medium containing a cocktail of mitotic inhibitors, resulting in the enrichment of differentiated neurons (NTera2-N).[36]

Western Blot Analysis

To prepare total protein extract for Western blot analysis, the cells and tissues were homogenized in RIPA lysis buffer composed of 50 mmol/L Tris-HCl (pH 7.5), 150 mmol/L NaCl, 1% Nonidet P-40, 0.5% sodium deoxycholate, 0.1% sodium dodecyl sulfate (SDS), and a cock-

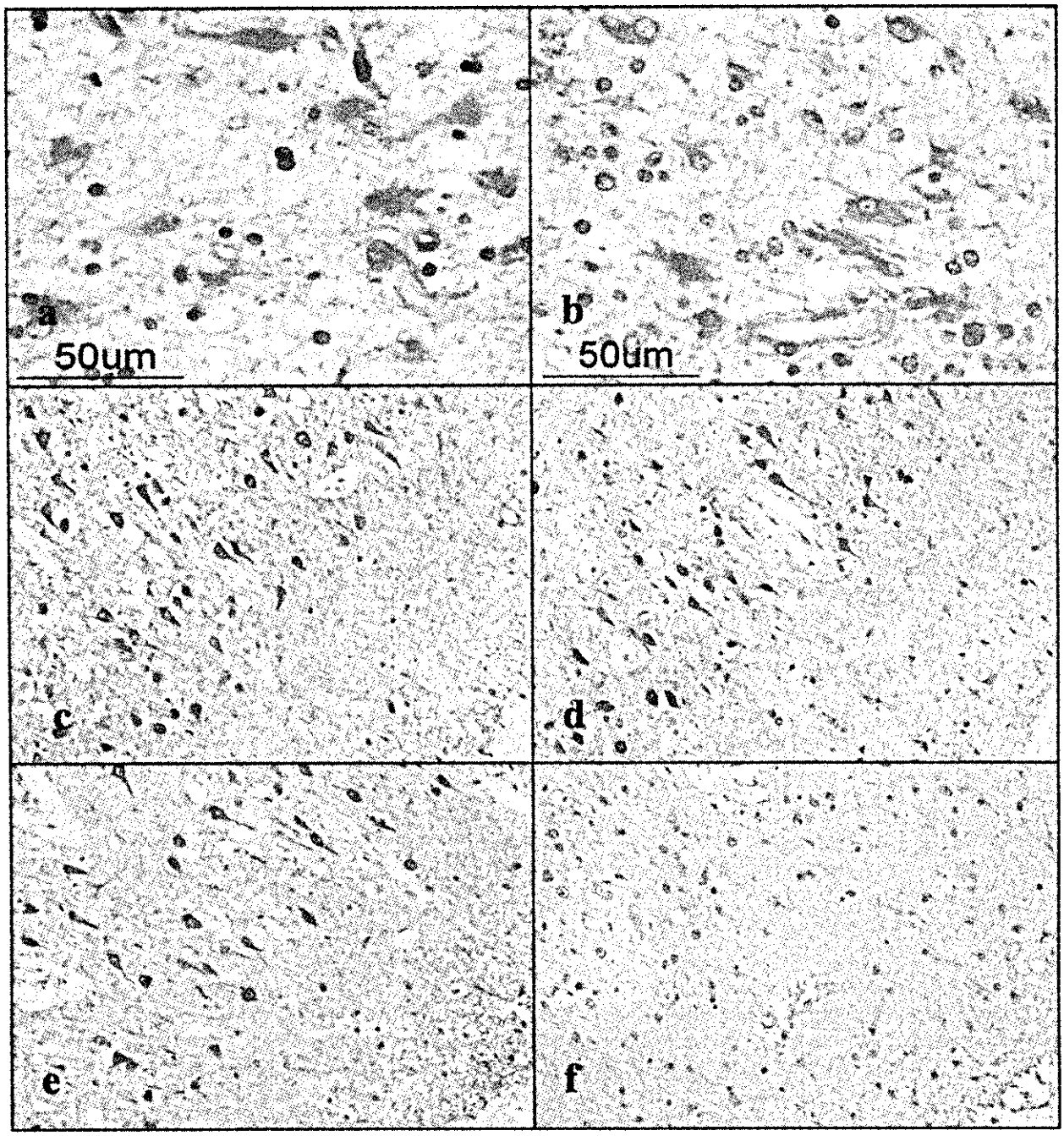

Figure 4. Expression of various 14-3-3 isoforms in reactive astrocytes and cortical neurons in MS brain. MS brain tissues were processed for immunohistochemical analysis using a battery of 14-3-3 isoform-specific antibodies. **a** to **f** represent the following: **a:** no. 744 MS, chronic active demyelinating lesions in the subcortical white matter of the frontal lobe (β). Reactive astrocytes are stained. **b:** No. 744 MS, chronic active demyelinating lesions in the subcortical white matter of the frontal lobe (ζ). Reactive astrocytes are stained. **c:** No. 744 MS, the cerebral cortex of the frontal lobe (γ). Cortical neurons are stained. **d:** No. 744 MS, the area corresponding to **c** (η). Cortical neurons are stained. **e:** No. 744 MS, the area corresponding to **c** (ζ). Cortical neurons are stained. **f:** No. 744 MS, the area corresponding to **c** (ϵ). Cortical neurons are devoid of staining.

tail of protease inhibitors (Roche Diagnositics, Mannheim, Germany), followed by centrifugation at 12,000 rpm at room temperature for 20 minutes. The supernatant was collected for separation on a 12% SDS-polyacrylamide gel electrophoresis (PAGE) gel and the protein concentration was determined by a Bradford assay kit (Bio-Rad, Hercules, CA). After gel electrophoresis, the protein was transferred onto nitrocellulose membranes and immunolabeled at room temperature overnight with a panel of anti-14-3-3 protein antibodies listed in Table 1. Then, the membranes were incubated at room temperature for 30 minutes with horseradish peroxidase-conjugated anti-rabbit IgG or anti-mouse IgG (Santa Cruz Biotechnology). The specific reaction was visualized with a Western blot detection system using a chemiluminescent substrate (Pierce, Rockford, IL). After the antibodies were stripped

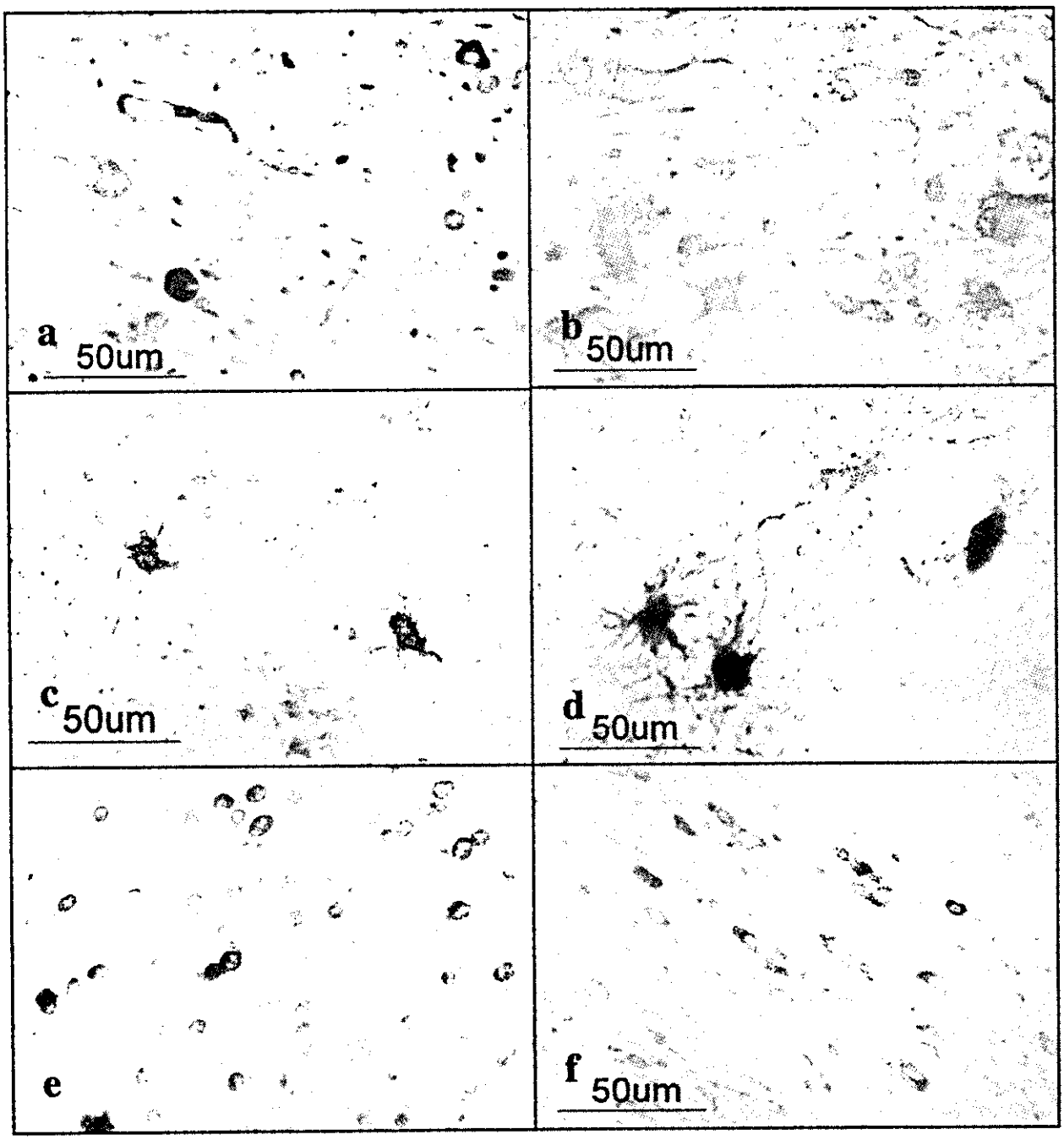

Figure 5. Expression of various 14-3-3 isoforms in reactive astrocytes, surviving oligodendrocytes, and injured axons in chronic demyelinating lesions of MS and in infarcted lesions. The brains of MS and non-MS control cases were processed for immunohistochemical analysis using a battery of 14-3-3 isoform-specific antibodies. **a** to **f** represent the following: **a:** no. 609 MS, chronic active demyelinating lesions in the medulla oblongata (γ). Disrupted axons are stained. **b:** No. 719 acute cerebral infarction, infarcted lesions in the parietal cerebral cortex (ϵ). Reactive astrocytes are stained. **c:** No. 791 MS, chronic inactive lesions in the pons (σ). Reactive astrocytes are stained. **d:** No. 719 acute cerebral infarction, infarcted lesions in the parietal cerebral cortex (σ). Reactive astrocytes are stained. **e:** No. 609 MS, chronic active demyelinating lesions in the periventricular white matter of the frontal lobe (θ). Surviving oligodendrocytes are stained. **f:** No. 744 MS, chronic active demyelinating lesions in the optic nerve (θ). Surviving oligodendrocytes are stained.

by incubating the membranes at 50°C for 30 minutes in stripping buffer composed of 62.5 mmol/L Tris-HCl (pH 6.7), 2% SDS, and 100 mmol/L 2-mercaptoethanol, the membranes were processed for relabeling with goat polyclonal antibody against human heat shock protein HSP60 (N-20; Santa Cruz Biotechnology) followed by incubation with horseradish peroxidase-conjugated anti-goat IgG (Santa Cruz Biotechnology). Densitometric analysis was performed using NIH image version 1.61 software to quantify the intensity of the immunoreactive bands.[36]

Immunoprecipitation Experiments

To prepare total protein extract for immunoprecipitation experiments, the cells were homogenized in M-PER lysis buffer (Pierce) with a cocktail of protease inhibitors fol-

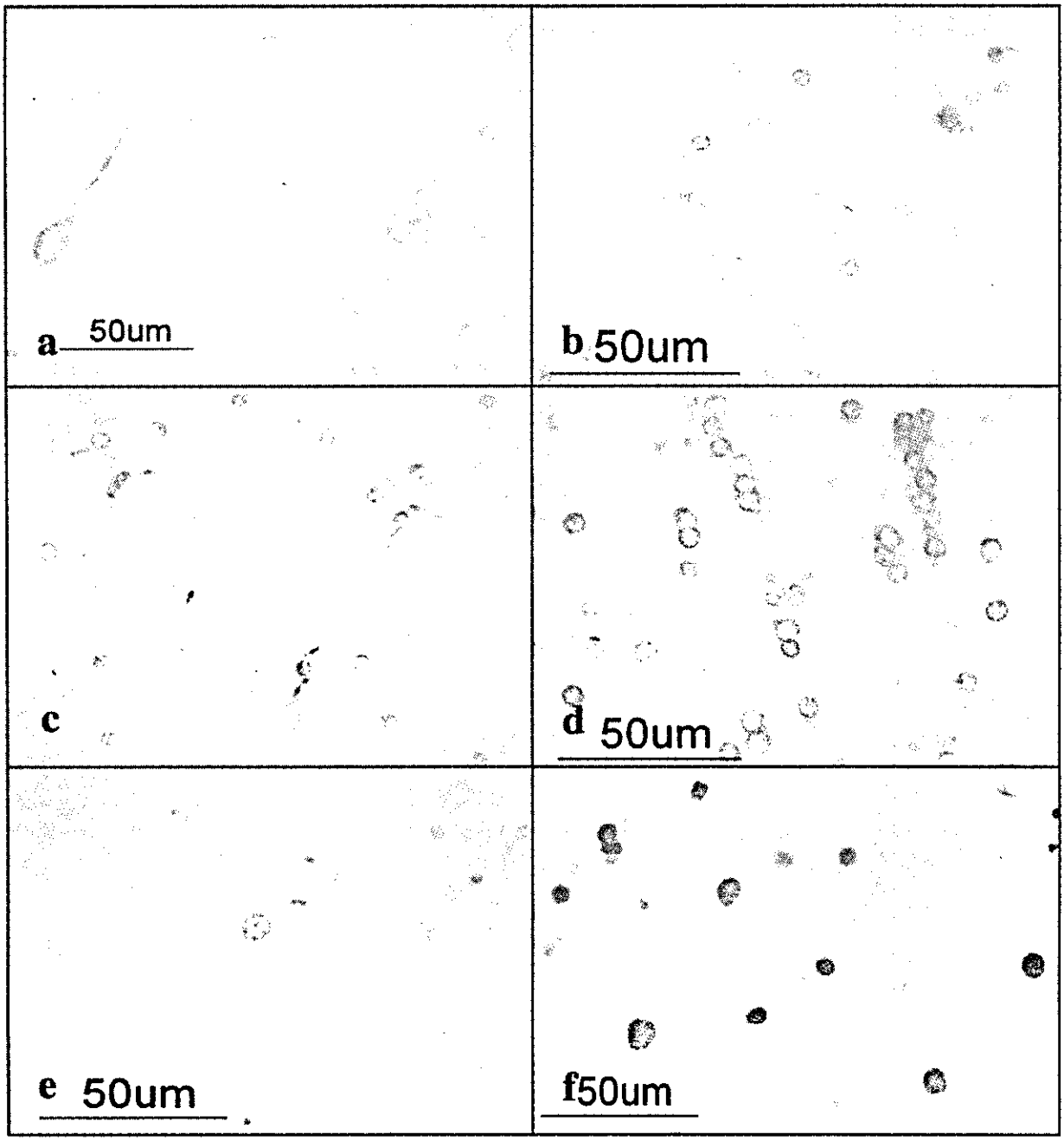

Figure 6. Expression of various 14-3-3 isoforms in neurons, astrocytes, oligodendrocytes, and microglia in non-MS brains. The brains of non-MS control cases were processed for immunohistochemical analysis using a battery of 14-3-3 isoform-specific antibodies. **a** to **f** represent the following: **a:** no. G9 neurologically normal subject, the frontal cerebral cortex (γ). Cortical neurons are stained. **b:** No. 523 schizophrenia, frontal cerebral cortex (ϵ). Astrocytes are stained. **c:** No. 826 schizophrenia, the frontal cerebral cortex (η). Microglia are stained. **d:** No. 786 acute cerebral infarction, the subcortical white matter of the parietal lobe (θ). Surviving oligodendrocytes are stained. **e:** No. G7 neurologically normal subject, the frontal cerebral cortex (σ). A few astrocytes are stained. **f:** No. 789 old cerebral infarction, the frontal cerebral cortex (η). The nuclei of reactive astrocytes are stained.

lowed by centrifugation at 12,000 rpm at room temperature for 20 minutes. After preclearance, the supernatant was incubated at 4°C for 1 hour with a panel of anti-14-3-3 protein antibodies or the same amount of normal rabbit IgG (Santa Cruz Biotechnology). It was then incubated with Protein G Sepharose (Amersham Bioscience, Piscataway, NJ). After several washes, the immunoprecipitates were processed for Western blot analysis using V9 antibody or mouse monoclonal antibody against GFAP (GA5; Nichrei).

Two-Dimensional Gel Electrophoresis and Mass Spectrometry Analysis

To prepare total protein extract for two-dimensional gel electrophoretic analysis, the cells were homogenized in

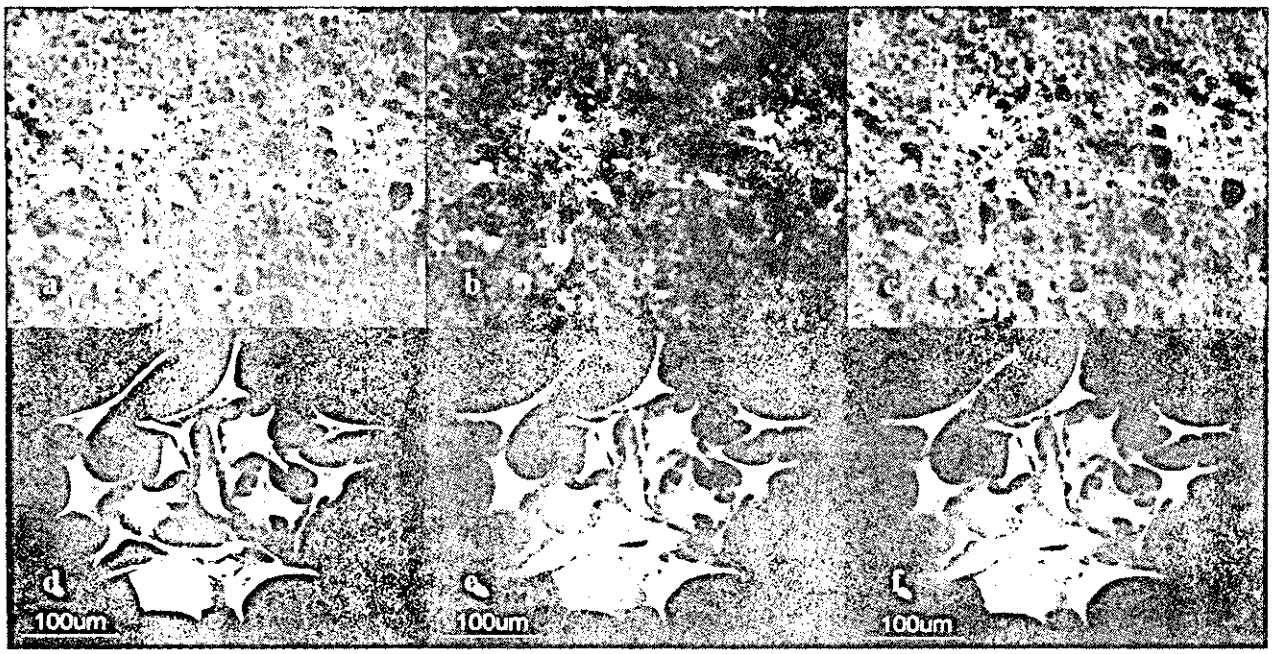

Figure 7. Co-expression of the 14-3-3 ε isoform and GFAP in reactive astrocytes in chronic demyelinating lesions of MS and in cultured human astrocytes. Cultured human astrocytes and MS brain tissues were processed for double immunolabeling with anti-GFAP antibody and ε isoform-specific antibody followed by labeling with fluorescein isothiocyanate- and rhodamine-conjugated secondary antibodies. **a** to **f** represent no. 744, chronic active demyelinating lesions in the subcortical white matter of the frontal lobe (**a–c**), cultured human astrocytes (AS-BW) (**d–f**), GFAP (**a**, **d**), ε (**b**, **e**), and the overlay (**c**, **f**).

rehydration buffer composed of 8 mol/L urea, 2% CHAPS, 0.5% carrier ampholytes (pH 4 to 6), 20 mmol/L dithiothreitol, 0.002% bromophenol blue, and a cocktail of protease inhibitors and phosphatase inhibitors (Sigma). Urea-soluble protein was separated by isoelectric focusing using the ZOOM IPGRunner system (Invitrogen) loaded with an immobilized pH 4.5 to 5.5 gradient strip. After the first dimension of isoelectric focusing, the protein was separated in the second dimension on a NuPAGE 4 to 12% polyacrylamide gel (Invitrogen). The gel was stained using Coomassie brilliant blue G-250 solution or the Silverquest silver staining kit (Invitrogen). It was transferred onto a polyvinylidene difluoride membrane for protein overlay and Western blot analysis. Spots of interest were excised from the gels, trypsinized, and processed for mass spectrometry (nanoESI-MS/MS) analysis followed by database searching using MASCOT software (Invitrogen Proteome, Yokohama, Japan).

Protein Overlay Analysis

To prepare the 14-3-3 protein-specific probe for protein overlay analysis, the open reading frame of the human 14-3-3ε isoform gene (YWHAE, GenBank accession No. NM_006761) was amplified from the cDNA of NTera2-N cells by the polymerase chain reaction using sense and anti-sense primers (5′atggatgatcgagaggatctggtg3′ and 5′tcactgattttcgtcttccacgtc3′). The polymerase chain reaction product was cloned into a prokaryotic expression vector pTrcHis-TOPO (Invitrogen). The expression of recombinant human 14-3-3ε protein having an N-terminal Xpress tag for detection (rh14-3-3ε) was induced in *Escherichia coli* by exposure to isopropyl β-thiogalactoside. The recombinant protein was further purified through a HiTrap chelating HP column (Amersham Bioscience) and by separation on a 12% SDS-PAGE gel. Recombinant human interferon-stimulated protein ISG15 fused to an N-terminal Xpress tag (rhISG15), a vimentin-binding protein in human cancer cells,[37] was prepared for the control probe. The polyvinylidene difluoride membrane on which the gel was blotted was incubated at room temperature overnight with 1 μg/ml rh14-3-3ε or rhISG15 probe, followed by immunolabeling with mouse monoclonal anti-Xpress antibody (Invitrogen) and horseradish peroxidase-conjugated anti-mouse IgG. After the probes and antibodies were stripped by incubating the membrane at 50°C for 30 minutes in stripping buffer, it was repeatedly relabeled with V9 antibody, GA5 antibody, or rabbit polyclonal antibodies specific for phosphorylated Ser-39, Ser-72, or Ser-83 epitopes of vimentin (Santa Cruz Biotechnology), followed by incubation with horseradish peroxidase-conjugated anti-mouse or rabbit IgG.

Results

Growth-Dependent Expression of 14-3-3 Isoforms in Cultured Human Astrocytes

To investigate the expression pattern of seven 14-3-3 isoforms in human neural cells, cultured human astrocytes, NTera2-N neurons, and U-373MG astrocytoma cells, all of which were incubated in 10% FBS-containing culture medium, were processed for Western blot analysis using a panel of isoform-specific antibodies or the antibodies broadly reactive against all of the isoforms listed in Table 1. Cultured human astrocytes, neurons, and astrocytoma cells, along with

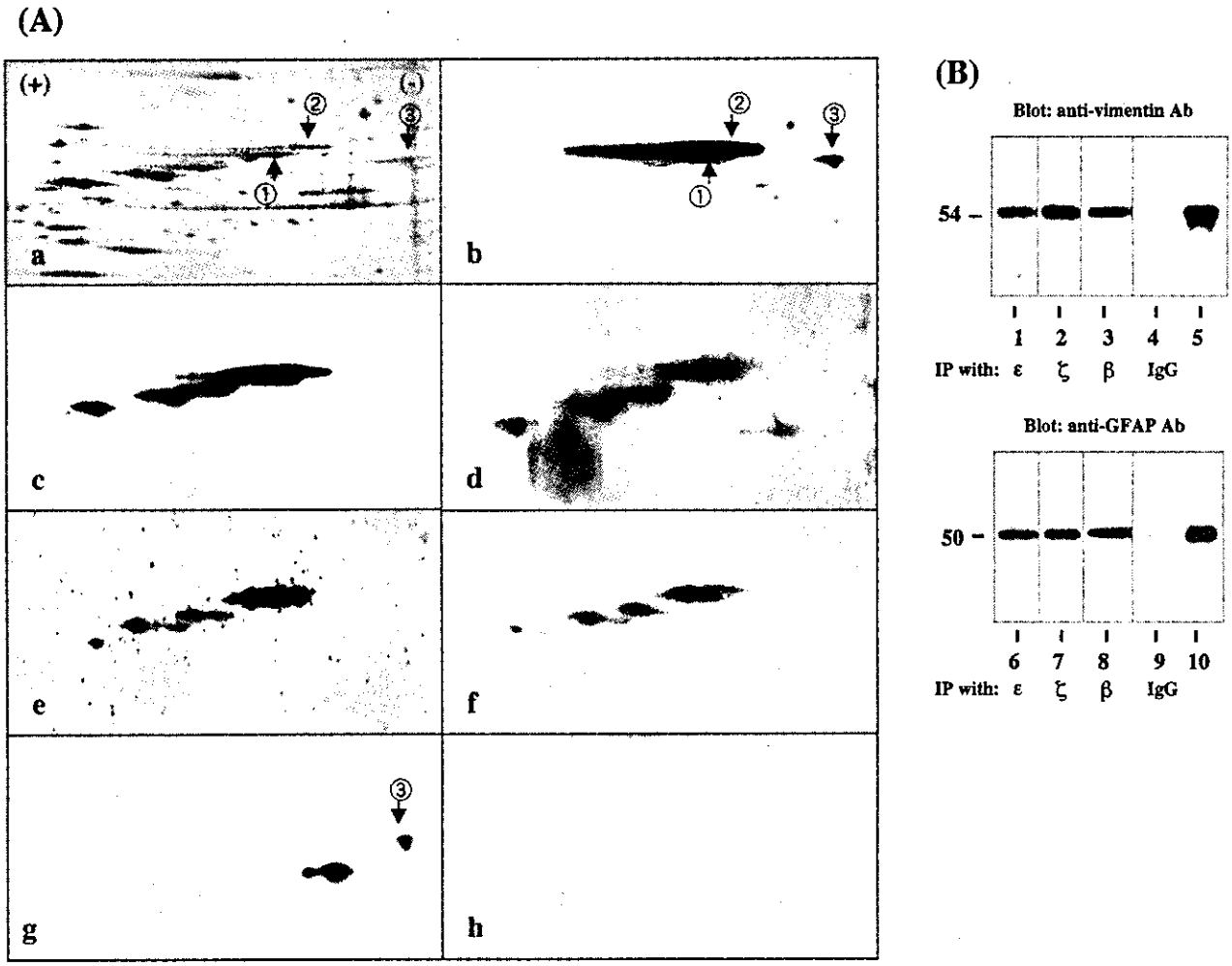

Figure 8. Two-dimensional gel electrophoresis and immunoprecipitation analysis of 14-3-3 ε isoform-binding proteins in cultured human astrocytes. **A:** Two-dimensional gel analysis. Human astrocytes (AS-BW) were incubated in 10% FBS-containing culture medium. Twenty-one μg of total protein extract was separated on a two-dimensional PAGE gel, transblotted onto a polyvinylidene difluoride membrane, and processed for overlay analysis with recombinant human 14-3-3ε protein possessing the Xpress tag (rh14-3-3ε) followed by labeling with anti-Xpress antibody. After the probe and antibody were stripped, the blot was repeatedly relabeled six times with the antibodies against GFAP, vimentin, and vimentin with specific phosphorylated serine epitopes, and with recombinant human interferon-stimulated protein ISG15 having the Xpress tag (rhISG15). **a** to **g** represent silver staining (**a**), rh14-3-3ε labeling followed by staining with anti-Xpress antibody (**b**), vimentin (**c**), vimentin with phosphorylated Ser-39 (**d**), vimentin with phosphorylated Ser-72 (**e**), vimentin with phosphorylated Ser-83 (**f**), GFAP (**g**), and rhISG15 labeling followed by staining with anti-Xpress antibody (**h**). Two major spots labeled with rh14-3-3ε and anti-vimentin antibody are named spot no. 1 and no. 2, while a spot labeled with rh14-3-3ε and anti-GFAP antibody is designated spot no. 3. Spots no. 1 and no. 2 were excised from the gel and processed for mass spectrometry (MS) analysis. **B:** Immunoprecipitation analysis. Total protein extract of cultured human astrocytes was immunoprecipitated with ε isoform-specific antibody (**lanes 1** and **6**), ζ isoform-specific antibody (**lanes 2** and **7**), β-isoform-specific antibody (**lanes 3** and **8**), with the same amount of normal rabbit IgG (**lanes 4** and **9**), or untreated with any antibodies (**lanes 5** and **10**; 2 μg of total protein extract before processing for immunoprecipitation). Then, the immunoprecipitates were processed for Western blot analysis using anti-vimentin (**top**) or anti-GFAP antibody (**bottom**).

human brain homogenate, expressed substantial levels of β, γ, ε, ζ, η, and θ isoforms (Figure 1, a to h; lanes 1 to 4). In contrast, the σ isoform was undetectable in human neural cells but was identified in HeLa cells (Figure 1i, lanes 1 to 5).

To study the effects of culture conditions on 14-3-3 protein levels, human astrocytes were incubated for 7 days in 10% FBS-containing culture medium or in the serum-free culture medium, which led to nearly complete growth arrest. The expression levels of β, γ, ε, ζ, η, and θ isoforms were elevated in human astrocytes incubated in the serum-containing growth-promoting condition. The expression was enhanced 3.3-, 1.6-, 2.2-, 10.0-, 18.7-, or 4.6-fold, respectively, compared with the levels under the serum-free growth-arrested condition when standardized against the levels of HSP60, a housekeeping gene product on the identical blots (Figure 2, a to c, e to g; top and bottom panels, lanes 1 and 2). The serum-induced up-regulation of 14-3-3 isoforms was also observed in a different culture of human astrocytes (Figure 2d, top and bottom panels, lanes 1 and 2) and mouse astrocytes in culture (Figure 2h, top and bottom panels, lanes 1 and 2; and additional data shown in Supplementary Figure 2 on The American Journal of Pathology website at *http://www.amjpathol.org*). These results indicate that cultured human astrocytes constitutively express all iso-

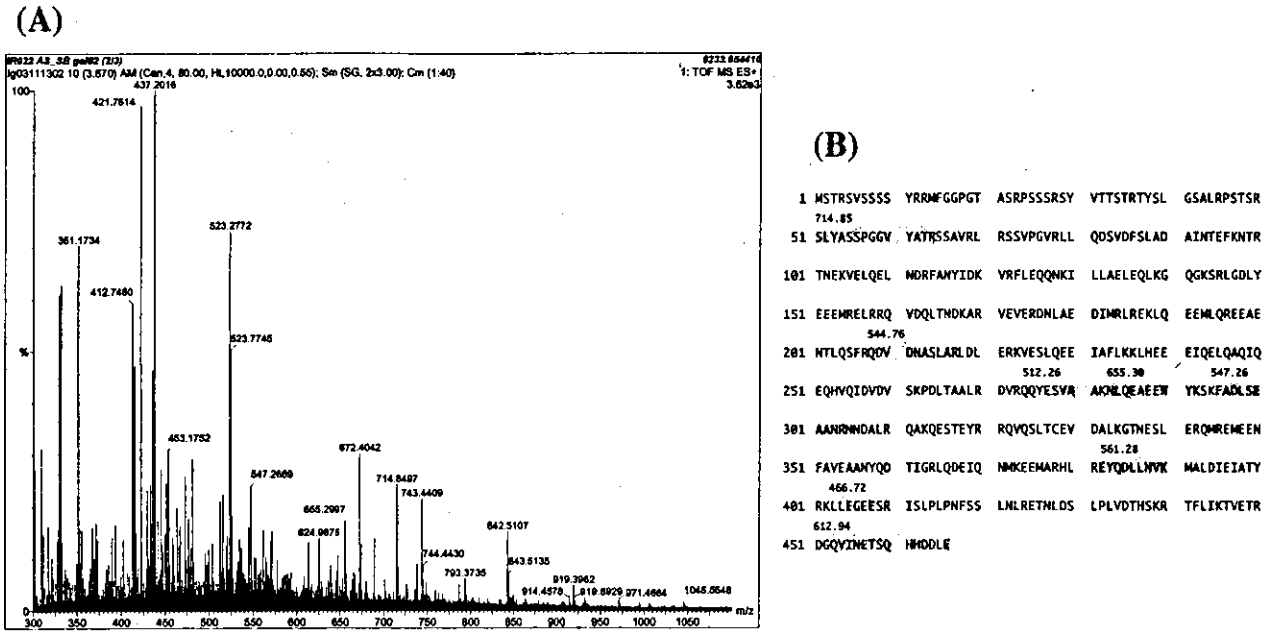

Figure 9. Mass spectrometry analysis of the 14-3-3 ε isoform-binding proteins in cultured human astrocytes. Spots no. 1 and no. 2 labeled with the rh14-3-3ε probe (Figure 8A, a and b) were excised from the gel, trypsinized, and processed for nanoESI-MS/MS analysis. **A:** The spectra of nanoESI-MS/MS analysis of spot no. 1. Each peak indicates individual peptide fragments. The position of several peaks was automatically numbered on the spectra. Peptides derived from the autolytic fragments of trypsin (eg, 412, 421, and 523) were omitted to be processed for further analysis. The peptide fragments were selected for MS analysis in order of their signal intensity. **B:** Amino acid sequence of human vimentin. Eight peptide fragments of spot no. 1 identified by nanoESI-MS/MS analysis (**shadowed**) showed a perfect match with the amino acid sequence encompassing residues 51 to 466 of vimentin. The number indicated on each fragment represents the position in the horizontal axis of the spectra (**A**).

forms except for σ, whose levels were elevated in a cell growth-dependent manner.

Differential Expression of 14-3-3 Isoforms in Reactive Astrocytes in Demyelinating Lesions of MS

To investigate the differential expression of seven 14-3-3 isoforms in MS lesions, the brain, spinal cord, and optic nerve of four progressive MS patients (no. 791, no. 744, no. 609, and no. 544) and 12 non-MS control cases were processed for immunohistochemistry using a panel of isoform-specific antibodies. In chronic active and inactive demyelinating lesions of MS, the majority of GFAP$^+$ hypertrophic astrocytes intensely expressed β, ε, ζ, and η isoforms, whereas a small population of reactive astrocytes displayed immunoreactivities against γ, θ, and σ isoforms (Table 2; Figure 3, a to e; Figure 4 a and b). Reactive astrocytes immunoreactive against the 14-3-3 protein exhibited the most dense accumulation at the lesion edge, although they were widely distributed in demyelinating lesions and in the normal appearing white matter. A glial scar was also intensely labeled with the antibodies against β, ε, ζ, and η isoforms (ε shown in Figure 3e and the others not shown). In MS and non-MS brains, a major population of cerebral cortical neurons constitutively expressed high levels of β, γ, ζ, and η isoforms, and to a lessor degree, θ isoform, whereas they hardly showed immunoreactivity for the σ isoform, and a small population of cerebral cortical neurons in MS and non-MS brains occasionally expressed weak immunoreactivity for the ε isoform, although these findings varied among brains for different cases (Table 2; Figure 4, c to f; and Figure 6). Disrupted, distorted, and swollen axons found in the active demyelinating lesions of MS exhibited strong immunoreactivity against γ and ζ isoforms (γ shown in Figure 5a and the other not shown).

A very small population of reactive astrocytes in demyelinating lesions of MS, which occasionally showed a binucleated morphology, intensely expressed the σ isoform, whose expression was not detected in cultured human astrocytes (Figure 5c). A number of reactive astrocytes that appeared in the ischemic lesions of cerebral infarction expressed strong immunoreactivity against ε, ζ, and η isoforms (Table 2; Figure 5b), and the σ isoform was again strongly expressed in a very small number of reactive astrocytes (Figure 5d). The immunoreactivity against the η isoform was often concentrated in the nuclear region of reactive astrocytes in MS lesions (not shown) and the ischemic lesions (Figure 6; a to f). Furthermore, some GFAP$^+$ astrocytes occasionally identified in the brains of schizophrenia and neurologically normal patients expressed ε and σ isoforms at variable levels (Table 2; Figure 6, b and e). CD68$^+$ macrophages and microglia, with the greatest accumulation identified in the center and edge of active demyelinating lesions of MS and necrotic lesions of cerebral infarction, expressed β, ζ, and η isoforms, whereas they did not show substantial immunoreactivity against ε, θ, or σ isoforms (Table 2; Figure 6c). CD3$^+$ lymphocytes found in the perivascular cuffs of active MS lesions expressed variable immunoreactivities for β and ζ isoforms (not shown). A substantial

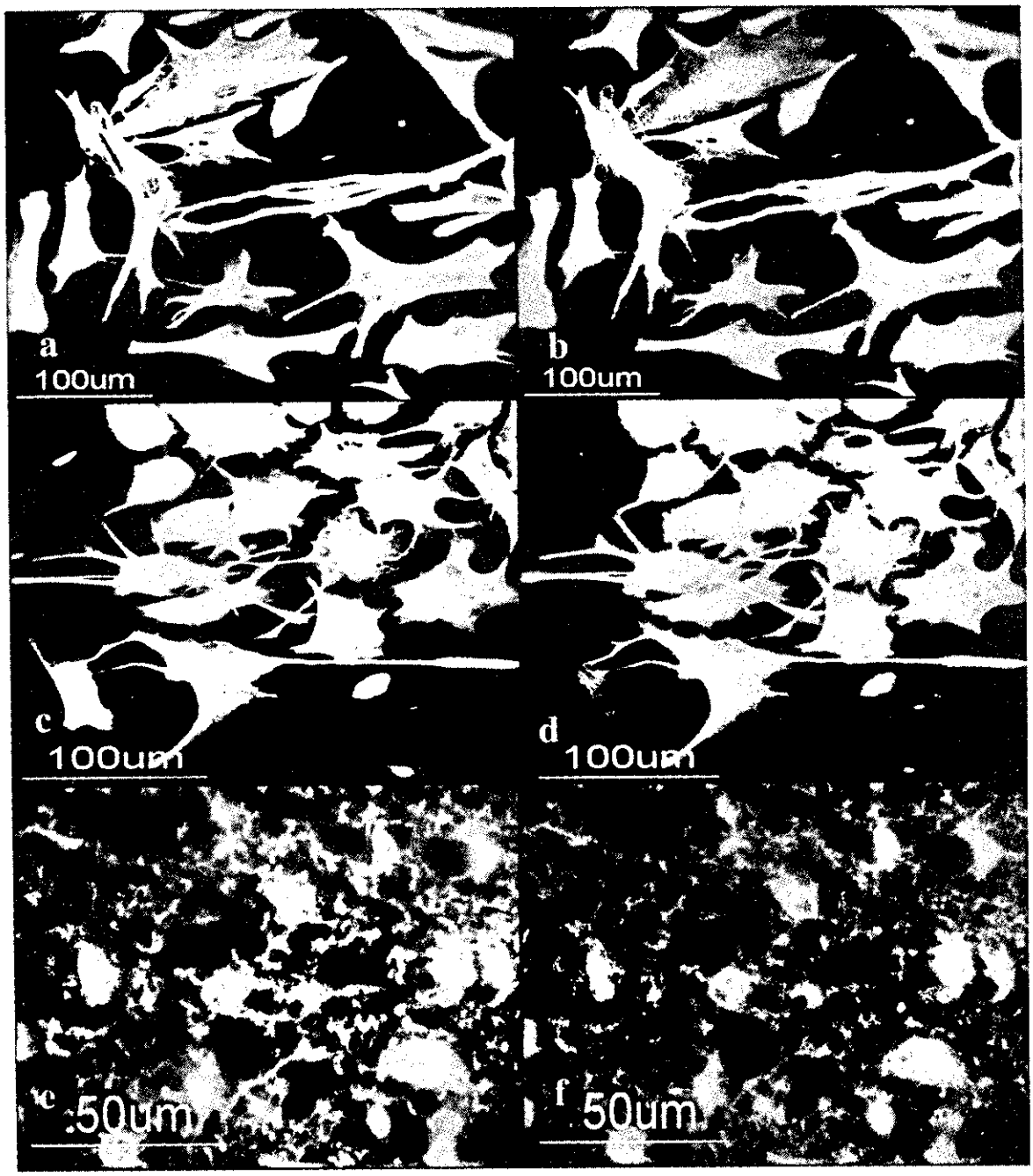

Figure 10. Co-expression of the 14-3-3 ϵ isoform and vimentin in cultured human astrocytes and reactive astrocytes in chronic demyelinating lesions of MS. Cultured human astrocytes and MS brain tissues were processed for double immunolabeling with anti-vimentin antibody and ϵ isoform-specific antibody or anti-GFAP antibody followed by labeling with fluorescein isothiocyanate- and rhodamine-conjugated secondary antibodies. **a** to **f** represent cultured human astrocytes (AS-BW) (**a–d**); no. 744, chronic active demyelinating lesions in the subcortical white matter of the frontal lobe (**e**, **f**); vimentin (**a**, **c**, **e**); ϵ (**b**, **f**); and GFAP (**d**).

population of oligodendrocytes, which survived in chronic active demyelinating lesions of MS and ischemic lesions of cerebral infarction, expressed intense immunoreactivity against θ isoform (Table 2; Figure 5, e and f; and Figure 6d). These results suggest that markedly up-regulated expression of the ϵ isoform is the most reliable marker for identifying reactive astrocytes in MS and non-MS brains. Co-expression of the ϵ isoform and GFAP was verified in reactive astrocytes in MS lesions (Figure 7; a to c) and cultured human astrocytes (Figure 7; d to f) by double immunolabeling.

Binding of the 14-3-3ϵ Isoform to Vimentin and GFAP in Cultured Human Astrocytes

To identify the binding partner of the 14-3-3 protein in human astrocytes, we performed a protein overlay anal-

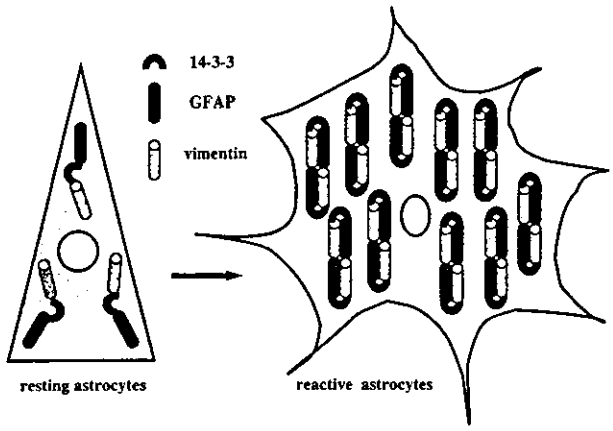

Figure 11. Putative role of the 14-3-3 protein in reactive gliosis in MS. Reactive gliosis is characterized by hypertrophy and proliferation of astrocytes associated with enhanced expression of GFAP (green) and vimentin (orange), which are co-polymerized in assembled filaments. Cultured human astrocytes expressed β, γ, ϵ, ζ, η, and θ isoforms, whose levels were markedly up-regulated under the growth-promoting culture condition, in which the 14-3-3 protein (red) interacted with vimentin (orange) and GFAP (green). These observations suggest that the 14-3-3 protein (red) might act as an adaptor that connects vimentin (orange) and GFAP (green) in reactive astrocytes at the site of demyelinating lesions in MS.

ysis using recombinant human 14-3-3ε protein with the Xpress tag (rh14-3-3ε) as a probe. Human astrocytes were incubated in 10% FBS-containing culture medium. Total protein extract was separated on a two-dimensional PAGE gel (Figure 8A, a) and transferred onto a polyvinylidene difluoride membrane (Figure 8A, b to h). The rh14-3-3ε probe strongly reacted with several spots on the blot, among which two major 54-kd spots were designated spots no. 1 and no. 2 (Figure 8A, b). In contrast, the rhISG15 probe did not react with these spots, excluding nonspecific binding of rh14-3-3ε via the Xpress tag (Figure 8A, h). Spots no. 1 and no. 2 were excised from the original gels, trypsinized, and processed for nanoESI-MS/MS analysis (Figure 9A). Among the peaks detected, eight peptide fragments derived from spot no. 1 and six from spot no. 2 showed a perfect match with the amino acid sequence covering residues 51 to 466 of human vimentin (Figure 9B), suggesting that these spots correspond to nearly full-length vimentin. Intense vimentin immunoreactivity was also identified in reactive astrocytes in demyelinating lesions of MS (Figure 3f). Furthermore, anti-vimentin monoclonal antibody reacted with spots no. 1 and no. 2, although this antibody labeled three additional, more acidic spots having smaller molecular weights (Figure 8A, c). The latter might represent post-translationally modified isoforms or degradation products of vimentin. Because vimentin is heavily phosphorylated at multiple serine residues in various mesenchymal cells, the phosphorylation state was characterized by repeated relabeling of the blot with three different antibodies specific for phosphorylated serine epitopes of vimentin. Phosphorylated Ser-39-, Ser-72-, and Ser-83-specific antibodies strongly reacted with spots no. 1 and no. 2, along with three additional spots unlabeled with rh14-3-3ε, suggesting that these serine residues are not involved in the interaction of the ε isoform with vimentin (Figure 8A, d to f). Protein overlay analysis using the rh14-3-3ε probe identified a distinct spot, designated spot no. 3 (Figure 8A, b). This spot was labeled with anti-GFAP antibody, indicating that GFAP is another binding partner of the 14-3-3 protein (Figure 8A, g). A more acidic spot having a smaller molecular weight immunoreactive for GFAP and weakly labeled with rh14-3-3ε might represent a post-translationally modified isoform or a degradation product of GFAP (Figure 8A, b and g). Vimentin and GFAP were detected in the immunoprecipitates of cultured human astrocyte protein extract, when the lysate was incubated with the ε, β, or ζ isoform-specific antibody (Figure 8B, top and bottom panels, lanes 1 to 3, 6 to 8). In contrast, only marginal bands were found in those with normal rabbit IgG (Figure 8B, top and bottom panels, lanes 4 and 9). Co-expression of the ε isoform with vimentin and GFAP was verified in cultured human astrocytes (Figure 10; a to d) and in reactive astrocytes in demyelinating lesions of MS (Figure 10, e and f) by double immunolabeling.

Discussion

The present study showed that seven 14-3-3 isoforms are differentially expressed in reactive astrocytes in demyelinating lesions of MS. Human astrocytes in culture also expressed β, γ, ϵ, ζ, η, and θ isoforms whose levels were markedly elevated under the growth-promoting culture condition. In demyelinating lesions of MS, the majority of GFAP$^+$ hypertrophic astrocytes intensely expressed β, ϵ, ζ, and η isoforms, although the expression of these isoforms was found in reactive astrocytes appearing in non-MS brains. Previous studies showed that the σ isoform expression is confined to differentiated squamous epithelial cells.[19,38] However, we found that some reactive astrocytes in MS and non-MS brains intensely expressed this isoform. Neurons constitutively expressed β, γ, ζ, and η isoforms but they did not constantly express ϵ or σ isoforms. Macrophages and microglia in MS and non-MS lesions intensely expressed β, ζ, and η isoforms, but they did not express ϵ, θ, or σ isoforms. A substantial population of oligodendrocytes, surviving in active demyelinating lesions of MS and ischemic lesions of cerebral infarction, intensely expressed the θ isoform, consistent with the expression of this isoform in the white matter of the developing rat CNS.[7] These observations are in agreement with our previous findings that the 14-3-3 protein is expressed not only in neurons but also in astrocytes, microglia, and oligodendrocytes in mouse brain cell cultures.[26] The present observations suggest that up-regulated expression of the ε isoform could be used as an immunohistochemical marker to identify reactive astrocytes at least in demyelinating lesions of MS and ischemic lesions of cerebral infarction. However, Lewy bodies in the Parkinson's disease brain[30] and a minor population of neurons in MS and non-MS brains express the ε isoform, indicating that this isoform is not astrocyte-specific.

The biological role of ε and σ isoforms in human astrocyte function remains unknown. Increasing evidence indicates that isoform-specific function regulates the devel-

opment and differentiation of neural and nonneural cells. Particularly, the ε isoform plays a role in the regulation of various cellular signaling events. The 14-3-3ε gene is deleted in the patients with Miller-Dieker syndrome, a human neuronal migration disorder presenting with the most severe form of lissencephaly (LIS) associated with facial abnormalities.[39] ε Isoform-deficient mice are defective in neuronal migration during brain development.[40] The multimolecular complex composed of the ε isoform, LIS1 and nudE nuclear distribution gene E homolog-like 1 (NUDEL) regulates the activity of dynein, a cytoplasmic motor protein, suggesting a role of ε in neuronal migration.[40] Somatic homozygous deletion of the 14-3-3ε gene is frequently found in small cell lung cancers, supporting the idea that the ε isoform serves as a tumor suppressor gene.[41] The 14-3-3ε isoform, by binding to the intracellular domain of the p75 neurotrophin receptor (NTR) in a NGF-dependent manner, promotes p75NTR-associated cell death executor (NADE)-mediated apoptosis.[42] During apoptosis, the ε protein is cleaved by caspase-3 at a cleavage site located in the C-terminal hydrophobic tail, where the amino acid sequence is highly variable among different 14-3-3 isoforms.[43] The ε isoform interacts with cdc25A and cdc25B phosphatases, key enzymes required for cell-cycle progression by activating cyclin-dependent kinases.[44] Phosphorylation-dependent interaction of the ε isoform with heat shock transcription factor HSF1 restricts the location of HSF1 in the cytoplasm by keeping it in an inactive form.[45] The ε isoform catalyzes the depolymerization and unfolding of mitochondrial precursor proteins in an ATP-dependent manner.[46] Based on these observations, we propose that the ε isoform plays a regulatory role in proliferation, apoptosis, and stress responses in reactive astrocytes.

The σ isoform constitutes a component of the G_2/M cell-cycle checkpoint machinery.[47] Exposure of the cells to DNA-damaging agents results in p53-dependent induction of the σ isoform, which in turn arrests the cells in the G_2/M phase by sequestering the cdc2-cyclin B1 complex in the cytoplasm.[48] Therefore, σ isoform-deficient cells are unable to maintain cell-cycle arrest.[47] Selective down-regulation of the σ isoform because of the hypermethylation of CpG islands in its promoter region is responsible for the malignant transformation of breast cancer cells,[49] whereas reduced expression of the σ isoform allows human epidermal keratinocytes to escape replicative senescence.[50] These observations raise the possibility that a population of reactive astrocytes with strong immunoreactivity against the σ isoform might represent the cells responding to DNA damage at the site of demyelinating lesions in MS and ischemic lesions of cerebral infarction.

Reactive gliosis is characterized by hypertrophy and proliferation of astrocytes associated with enhanced expression of GFAP and vimentin, accompanied by increased production of growth factors, cytokines, neuropeptides, and extracellular matrix molecules.[51,52] Astrocytes play a role in the repair of the blood-brain barrier, protection of neurons from glutamate excitotoxicity, and enhancement of neuronal survival by supplying neurotrophic factors.[53] On the other hand, reactive astrocytes strongly inhibit neurite outgrowth by forming glial scars after CNS injury and inflammation.[53,54] Through protein overlay and nanoESI-MS/MS analysis, we showed that vimentin is the major 14-3-3 protein-interacting protein expressed in cultured human astrocytes. Consistent with previous observations,[55,56] we identified vimentin expression in reactive astrocytes in demyelinating lesions of MS. Astrocytes isolated from vimentin-deficient mice possess an abnormal filamentous network of GFAP.[57,58] Furthermore, mice lacking vimentin and GFAP do not form proper glial scars after CNS injury, indicating that the type III IF family proteins play a pivotal role in cytoskeletal organization in astrocytes.[59]

In our study, the rh14-3-3ε probe strongly reacted with two distinct spots named no. 1 and no. 2 among five phosphovimentin-immunoreactive spots on the blot. Vimentin was immunoprecipitated with the ζ and β isoforms along with ε. These observations suggest that the interaction between vimentin and the 14-3-3 protein is not isoform-specific, and that the 14-3-3 protein-binding domain in vimentin might not include phosphorylated Ser-39, Ser-72, and Ser-83 epitopes. Protein overlay analysis identified GFAP as another binding partner of the 14-3-3ε isoform. Immunoprecipitation experiments verified the interaction between GFAP and the ε, ζ, or β isoform. However, a different spot strongly immunoreactive against GFAP but much weakly labeled with rh14-3-3ε was identified on the two-dimensional gel blot. This suggests that a substantial pool of cytoplasmic vimentin and GFAP proteins steadily interact with the 14-3-3 protein in human astrocytes.

Our observations raise the possibility that the 14-3-3 protein acts as an adaptor that connects vimentin and GFAP in cultured human astrocytes (Figure 11). Previous studies showed that vimentin and GFAP are co-expressed and co-polymerized in assembled filaments in astrocytes,[58,60] supporting the view that the 14-3-3 protein not only bridges vimentin and GFAP one by one, but also bundles both of them in the same assembled filaments. All these proteins are expressed at much higher levels in reactive astrocytes, which require more efforts to coordinate the IF network compared with resting astrocytes (Figure 11). Several other binding partner candidates for vimentin in astrocytes include α-crystallin, which inhibits the *in vitro* assembly of GFAP,[61] and the multiple endocrine neoplasia type 1 (MEN1) gene product named menin, which binds to vimentin and GFAP in glioma cells.[62] The 14-3-3γ isoform interacts with F-actin and Raf kinase in cultured mouse astrocytes, indicating its role in cytoskeletal rearrangement during cell growth and division.[63,64] Importantly, a recent study using COS-7 cells overexpressing the 14-3-3 protein showed that phosphorylated vimentin binds to the 14-3-3 protein and limits the interaction of 14-3-3 with other 14-3-3-binding partners, thereby modulating Raf-dependent intracellular signaling.[65] This study also found that vimentin does not have typical consensus 14-3-3-binding motifs.[65] However, a close interaction of the 14-3-3 protein with phosphorylated vimentin affects the phosphorylation and dephosphorylation state of vimentin.[65] Site-specific phosphorylation of vimentin and GFAP is mediated by

a range of protein kinases, including Rho kinase, cdc2 kinase, Ca^{2+} calmodulin-dependent kinase II, protein kinases A and C, and Aurora-B kinase.[60,66–69] They coordinately regulate dynamic equilibrium between the assembly and disassembly of IF proteins during mitosis.[60,66–69] Furthermore, these kinases are identified as binding partners for the 14-3-3 protein.[1–3] Therefore, our observations suggest that the 14-3-3 protein plays a role in the organization of IF proteins and IF-related kinases during conversion from resting astrocytes to reactive astrocytes. A role for 14-3-3 protein in IF dynamics is supported by our preliminary observations that suggest the effects of difopein,[70] a specific inhibitor of 14-3-3 protein/ligand interaction, on the morphological characteristics of cultured human astrocytes.

Acknowledgments

We thank Dr. Mitsuru Kawai, Department of Neurology, National Center Hospital for Mental, Nervous, and Muscular Disorders, NCNP, Tokyo, Japan, for providing information about MS patients; Dr. Toshikazu Murakami, Department of Pathology, Kohnodai Hospital, NCNP, Chiba, Japan, for providing the brains of neurologically normal controls; Drs. Kazuhiko Watabe and S.U. Kim, University of British Columbia, Vancouver, BC, Canada, for providing cultured fetal human astrocytes; and Dr. Masashi Fukuda, Invitrogen Proteome, Yokohama, Japan, for his help in nanoESI-MS/MS analysis.

References

1. Fu H, Subramanian RR, Masters SC: 14-3-3 proteins: structure, function, and regulation. Annu Rev Pharmacol Toxicol 2000, 40:617–647
2. van Hemert MJ, Steensma HY, van Heusden GPH: 14-3-3 proteins: key regulators of cell division, signaling and apoptosis. Bioessays 2001, 23:936–947
3. Aitken A, Baxter H, Dubois T, Clokie S, Mackie S, Mitchell K, Peden A, Zemlickova E: 14-3-3 proteins in cell regulation. Biochem Soc Trans 2002, 30:351–360
4. Berg D, Holzmann C, Riess O: 14-3-3 proteins in the nervous system. Nature Rev Neurosci 2002, 4:752–762
5. Boston PF, Jackson P, Kyonoch PAM, Thompson RJ: Purification, properties, and immunohistochemical localisation of human brain 14-3-3 protein. J Neurochem 1982, 38:1466–1474
6. Watanabe M, Isobe T, Ichimura T, Kuwano R, Takahashi Y, Kondo H: Molecular cloning of rat cDNAs for β and γ subtypes of 14-3-3 protein and developmental changes in expression of their mRNAs in the nervous system. Mol Brain Res 1993, 17:135–146
7. Watanabe M, Isobe T, Ichimura T, Kuwano R, Takahashi Y, Kondo H, Inoue Y: Molecular cloning of rat cDNAs for the ζ and θ subtypes of 14-3-3 protein and differential distributions of their mRNAs in the brain. Mol Brain Res 1994, 25:113–121
8. Muslin AJ, Xing H: 14-3-3 proteins: regulation of subcellular localization by molecular interference. Cell Signal 2000, 12:703–709
9. Yaffe MB: How do 14-3-3 proteins work?—gatekeeper phosphorylation and the molecular anvil hypothesis. FEBS Lett 2002, 513:53–57
10. Tzivion G, Avruch J: 14-3-3 proteins: active cofactors in cellular regulation by serine/threonine phosphorylation. J Biol Chem 2002, 277:3061–3064
11. Zhai J, Lin H, Shamim M, Schlaepfer WW, Cañete-Soler R: Identification of a novel interaction of 14-3-3 with p190RhoGEF. J Biol Chem 2001, 276:41318–41324
12. Dai J-G, Murakami K: Constitutively and autonomously active protein kinase C associated with 14-3-3 ζ in the rodent brain. J Neurochem 2003, 84:23–34
13. Broadie K, Rushton E, Skoulakis EMC, Davis RL: Leonardo, a Drosphila 14-3-3 protein involved in learning, regulates presynaptic function. Neuron 1997, 19:391–402
14. Meller N, Liu Y-C, Collins TL, Bonnefoy-Bérard N, Naier G, Isakov N, Altman A: Direct interaction between protein kinase Cθ (PKCθ) and 14-3-3τ in T cells: 14-3-3 overexpression results in inhibition of PKCθ translocation and function. Mol Cell Biol 1996, 16:5782–5791
15. Craparo A, Freund R, Gustafson TA: 14-3-3 (ε) interacts with the insulin-like growth factor I receptor and insulin receptor substrate I in a phosphoserine-dependent manner. J Biol Chem 1997, 272:11663–11669
16. Vincenz C, Dixit VM: 14-3-3 proteins associate with A20 in an isoform-specific manner and function both as chaperone and adaptor molecules. J Biol Chem 1996, 271:20029–20034
17. Wakui H, Wright APH, Gustafsson J-A, Zilliacus J: Interaction of the ligand-activated glucocorticoid receptor with the 14-3-3η protein. J Biol Chem 1997, 272:8153–8156
18. Hashiguchi M, Sobue K, Paudel HK: 14-3-3ζ is an effector of tau protein phosphorylation. J Biol Chem 2000, 275:25247–25254
19. Leffers H, Madsen P, Rasmussen HH, Honoré B, Andersen AH, Walbum E, Vandekerckhove J, Celis JE: Molecular cloning and expression of the transformation sensitive epithelial marker stratifin. A member of a protein family that has been involved in the protein kinase C signaling pathway. J Mol Biol 1993, 231:982–998
20. Martin H, Rostas J, Patel Y, Aitken A: Subcellular localisation of 14-3-3 isoforms in rat brain using specific antibodies. J Neurochem 1994, 63:2259–2265
21. Baxter HC, Liu W-G, Forster JL, Aitken A, Fraser JR: Immunolocalisation of 14-3-3 isoforms in normal and scrapie-infected murine brain. Neuroscience 2002, 109:5–14
22. Hsich G, Kenney K, Gibbs Jr CJ, Lee KH, Harrington MG: The 14-3-3 brain protein in cerebrospinal fluid as a marker for transmissible spongiform encephalopathies. N Engl J Med 1996, 335:924–930
23. Zerr I, Bodemer M, Gefeller O, Otto M, Poser S, Wiltfang J, Windl O, Kretzschmar HA, Weber T: Detection of 14-3-3 protein in the cerebrospinal fluid supports the diagnosis of Creutzfeldt-Jakob disease. Ann Neurol 1998, 43:32–40
24. Wiltfang J, Otto M, Baxter HC, Bodemer M, Steinacker P, Bahn E, Zerr I, Kornhuber J, Kretzschmar HA, Poser S, Rüther E, Aitken A: Isoform pattern of 14-3-3 proteins in the cerebrospinal fluid of patients with Creutzfeldt-Jakob disease. J Neurochem 1999, 73:2485–2490
25. Richard M, Biacabe A-G, Streichenberger N, Ironside JW, Mohr M, Kopp N, Perret-Liaudet A: Immunohistochemical localization of 14.3.3 ζ protein in amyloid plaques in human spongiform encephalopathies. Acta Neuropathol 2003, 105:296–302
26. Satoh J, Kurohara K, Yukitake M, Kuroda Y: The 14-3-3 protein detectable in the cerebrospinal fluid of patients with prion-unrelated neurological diseases is expressed constitutively in neurons and glial cells in culture. Eur Neurol 1999, 41:216–225
27. Satoh J, Yukitake M, Kurohara K, Takashima H, Kuroda Y: Detection of the 14-3-3 protein in the cerebrospinal fluid of Japanese multiple sclerosis patients presenting with severe myelitis. J Neurol Sci 2003, 212:11–20
28. Layfield R, Fergusson J, Aitken A, Lowe J, Landon M, Mayer RJ: Neurofibrillary tangles of Alzheimer's disease brains contain 14-3-3 proteins. Neurosci Lett 1996, 209:57–60
29. Agarwal-Mawal A, Qureshi HY, Cafferty PW, Yuan Z, Han D, Lin R, Paudel HK: 14-3-3 connects glycogen synthase kinase-3β to tau within a brain microtubule-associated tau phosphorylation complex. J Biol Chem 2003, 278:12722–12728
30. Berg D, Riess O, Bornemann A: Specification of 14-3-3 proteins in Lewy bodies. Ann Neurol 2003, 54:135
31. Ostrerova N, Petrucelli L, Farrer M, Mehta N, Choi P, Hardy J, Wolozin B: α-Synuclein shares physical and functional homology with 14-3-3 proteins. J Neurosci 1999, 19:5782–5791
32. Xu J, Kao S-Y, Lee FJS, Song W, Jin L-W, Yanker BA: Dopamine-dependent neurotoxicity of α-synuclein: a mechanism for selective neurodegeneration in Parkinson disease. Nat Med 2002, 8:600–606
33. Chen H-K, Fernandez-Funez P, Acevedo SF, Lam YC, Kaytor MD, Fernandez MH, Aitken A, Skoulakis EMC, Orr HT, Botas J, Zoghbi HY: Interaction of Akt-phosphorylated ataxin-1 with 14-3-3 mediates neurodegeneration in spinocerebellar ataxia type 1. Cell 2003, 113:457–468

34. Malaspina A, Kaushik N, de Belleroche J: A 14-3-3 mRNA is upregulated in amyotrophic lateral sclerosis spinal cord. J Neurochem 2000, 75:2511–2520
35. Carpenter MK, Cui X, Hu Z-Y, Jackson J, Sherman S, Seiger Å, Wahlberg LU: In vitro expansion of a multipotent population of human neural progenitor cells. Exp Neurol 1999, 158:262–278
36. Satoh J, Kuroda Y: Differential gene expression between human neurons and neuronal progenitor cells in culture: an analysis of arrayed cDNA clones in NTera2 human embryonal carcinoma cell line as a model system. J Neurosci Methods 2000, 94:155–164
37. Loeb KR Haas AL: Conjugates of ubiquitin cross-reactive protein distribute in a cytoskeletal pattern. Mol Cell Biol 1994, 14:8408–8419
38. Prasad GL, Valverius EM, McDuffie E, Cooper HL: Complementary DNA cloning of a novel epithelial cell marker protein, HME1, that may be down-regulated in neoplastic mammary cells. Cell Growth Differ 1992, 3:507–513
39. Cardoso C, Leventer RJ, Ward HL, Toyo-oka K, Chung J, Gross A, Martin CL, Allanson J, Pilz DT, Olney AH, Mutchinick OM, Hirotsune S, Wynshaw-Boris A, Dobyns WB, Ledbetter DH: Refinement of a 400-kb critical region allows genotypic differentiation between isolated lissencephaly, Miller-Dieker syndrome, and other phenotypes secondary to deletions of 17p13.3. Am J Hum Genet 2003, 72:918–930
40. Toyo-Oka K, Shinoya A, Gambello MJ, Cardoso C, Leventer R, Ward HL, Ayala R, Tsai L-H, Dobyns W, Ledbetter D, Hirotsune S, Wynshaw-Boris A: 14-3-3ϵ is important for neuronal migration by binding to NUDEL: a molecular explanation for Miller-Dieker syndrome. Nat Genet 2003, 34:274–285
41. Konishi H, Nakagawa T, Harano T, Mizuno K, Saito H, Masuda A, Matsuda H, Osada H, Takahashi T: Identification of frequent G_2 checkpoint impairment and a homozygous deletion of 14-3-3ϵ at 17p13.3 in small cell lung cancers. Cancer Res 2002, 62:271–276
42. Kimura MT, Irie S, Shoji-Hoshino S, Mukai J, Nadano D, Oshimura M, Sato T-A: 14-3-3 is involved in p75 neurotrophin receptor-mediated signal transduction. J Biol Chem 2001, 276:17291–17300
43. Won J, Kim DY, La M, Kim D, Meadows GG, Joe CO: Cleavage of 14-3-3 protein by caspase-3 facilitates Bad interaction with Bcl-x(L) during apoptosis. J Biol Chem 2003, 278:19347–19351
44. Conklin DS, Galaktionov K, Beach D: 14-3-3 proteins associate with cdc25 phosphatases. Proc Natl Acad Sci USA 1995, 92:7892–7896
45. Wang X, Grammatikakis N, Siganou A, Calderwood SK: Regulation of molecular chaperone gene transcription involves the serine phosphorylation, 14-3-3ϵ binding, and cytoplasmic sequestration of heat shock factor 1. Mol Cell Biol 2003, 23:6013–6026
46. Alam R, Hachiya N, Sakaguchi M, Kawabata S-I, Iwanaga S, Kitajima M, Mihara K, Omura T: cDNA cloning and characterization of mitochondrial import stimulation factor (MSF) purified from rat liver cytosol. J Biochem 1994, 116:416–425
47. Chan TA, Hermeking H, Lengauer C, Kinzler KW, Vogelstein B: 14-3-3σ is required to prevent mitotic catastrophe after DNA damage. Nature 1999, 401:616–620
48. Hermeking H, Lengauer C, Polyak K, He T-C, Zhang L, Thiagalingam S, Kinzler KW, Vogelstein B: 14-3-3σ is a p53-regulated inhibitor of G2/M progression. Mol Cell 1997, 1:3–11
49. Ferguson AT, Evaron E, Umbricht CB, Pandita TK, Chan TA, Hermeking H, Marks JR, Lambers AR, Futreal PA, Stampfer MR, Sukumar S: High frequency of hypermethylation at the 14-3-3 σ locus leads to gene silencing in breast cancer. Proc Natl Acad Sci USA 2000, 97:6049–6054
50. Dellambra E, Golisano O, Bondanza S, Siviero E, Lacal P, Molinari M, D'Atri S, De Luca M: Downregulation of 14-3-3σ prevents clonal evolution and leads to immortalization of primary human keratinocytes. J Cell Biol 2000, 149:1117–1129
51. Mucke L, Eddleston M: Astrocytes in infectious and immune-mediated diseases of the central nervous system. EMBO J 1993, 7:1226–1232
52. Ridet JL, Malhotra SK, Privat A, Gage FH: Reactive astrocytes: cellular and molecular cues to biological function. Trends Neurosci 1997, 20:570–577
53. Bush TG, Puvanachandra N, Horner CH, Polito A, Ostenfeld T, Svendsen CN, Mucke L, Johnson MH, Sofroniew MV: Leukocyte infiltration, neuronal degeneration, and neurite outgrowth after ablation of scar-forming, reactive astrocytes in adult transgenic mice. Neuron 1999, 23:297–308
54. Menet V, Ribotta MGY, Chauvet N, Drian MJ, Lannoy J, Colucci-Guyon E, Privat A: Inactivation of the glial fibrillary acidic protein gene, but not that of vimentin, improves neuronal survival and neurite growth by modifying adhesion molecule expression. J Neurosci 2001, 21:6147–6158
55. Yamada T, Kawamata T, Walker DG, McGeer PL: Vimentin immunoreactivity in normal and pathological human brain tissues. Acta Neuropathol 1992, 84:157–162
56. Holley JE, Gveric D, Newcombe J, Cuzner ML, Gutowski NJ: Astrocyte characterization in the multiple sclerosis glial scar. Neuropathol Appl Neurobiol 2003, 29:434–444
57. Galou M, Solucci-Guyon E, Ensergueix D, Ridet J-L, Robotta MGY, Privat A, Babinet C, Dupouey P: Disrupted glial fibrillary acidic protein network in astrocytes from vimentin knockout mice. J Cell Biol 1996, 133:853–863
58. Eliasson C, Sahlgrens C, Berthold C-H, Stakeberg J, Celis JE, Betsholtz C, Eriksson JE, Pekny M: Intermediate filament protein partnership in astrocytes. J Biol Chem 1999, 274:23996–24006
59. Pekny M, Johansson B, Eliasson C, Stakeberg J, Wallén Å, Perlmann T, Lendahl U, Betsholtz C, Berthold C-H, Frisén J: Abnormal reaction to central nervous system injury in mice lacking glial fibrillary acidic protein and vimentin. J Cell Biol 1999, 145:503–514
60. Inagaki M, Nakamura Y, Takeda M, Nishimura T, Inagaki N: Glial fibrillary acidic protein: dynamic property and regulation by phosphorylation. Brain Pathol 1994, 4:239–243
61. Nicholl ID, Quinlan RA: Chaperone activity of α-crystallins modulates intermediate filament assembly. EMBO J 1994, 13:945–953
62. Lopez-Egido JR, Cunningham J, Berg M, Oberg K, Bongcam-Rudloff E, Gobl AE: Menin's interaction with glial fibrillary acidic protein and vimentin suggests a role for the intermediate filament network in regulating menin activity. Exp Cell Biol 2002, 278:175–183
63. Chen XQ, Yu ACH: The association of 14-3-3γ and actin plays a role in cell division and apoptosis in astrocytes. Biochem Biophys Res Commun 2002, 296:657–663
64. Chen XQ, Chen JG, Zhang Y, Hsiao WWL, Yu ACH: 14-3-3γ is upregulated by in vitro ischemia and binds to protein kinase Raf in primary cultures of astrocytes. Glia 2003, 42:315–324
65. Tzivion G, Luo Z-J, Avruch J: Calyculin A-induced vimentin phosphorylation sequesters 14-3-3 and displaces other 14-3-3 partners in vivo. J Biol Chem 2000, 275:29772–29778
66. Tsujimura K, Tanaka J, Ando S, Matsuoka Y, Kusubata M, Sugiura H, Yamauchi T, Inagaki M: Identification of phosphorylation sites on glial fibrillary acidic protein for cdc2 kinase and Ca^{2+}-calmodulin-dependent protein kinase II. J Biochem 1994, 116:426–434
67. Goto H, Kosako H, Tanabe K, Yanagida M, Sakurai M, Amano M, Kaibuchi K, Inagaki M: Phosphorylation of vimentin by Rho-associated kinase at a unique amino-terminal site that is specifically phosphorylated during cytokinesis. J Biol Chem 1998, 273:11728–11738
68. Takemura M, Gomi H, Colucci-Guyon E, Itohara S: Protective role of phosphorylation in turnover of glial fibrillary acidic protein in mice. J Neurosci 2002, 22:6972–6979
69. Goto H, Yasui Y, Kawajiri A, Nigg EA, Terada Y, Tatsuka M, Nagata K-I, Inagaki M: Aurora-B phosphorylates the cleavage furrow-specific vimentin phosphorylation in the cytokinetic process. J Biol Chem 2003, 278:8526–8530
70. Masters SC, Fu H: 14-3-3 proteins mediate an essential anti-apoptotic signal. J Biol Chem 2001, 276:45193–45200

A Structural Basis for the Association of DAP12 with Mouse, but Not Human, NKG2D[1]

David B. Rosen,* Manabu Araki,[2†] Jessica A. Hamerman,* Taian Chen,* Takashi Yamamura,[†] and Lewis L. Lanier[3]*

Prior studies have revealed that alternative mRNA splicing of the mouse *NKG2D* gene generates receptors that associate with either the DAP10 or DAP12 transmembrane adapter signaling proteins. We report that NKG2D function is normal in human patients lacking functional DAP12, indicating that DAP10 is sufficient for human NKG2D signal transduction. Further, we show that human NKG2D is incapable of associating with DAP12 and provide evidence that structural differences in the transmembrane of mouse and human NKG2D account for the species-specific difference for this immune receptor. *The Journal of Immunology,* **2004, 173: 2470–2478.**

The activity of NK cells is regulated by a balance of positive and negative signals transduced, respectively, via activating and inhibitory cell surface receptors (1, 2). The activating receptor NKG2D, a C type-like lectin and type II transmembrane (TM)[4] protein (3), is expressed on all NK cells, γδ TCR$^+$ T cells, and human CD8$^+$ T cells and is induced on activated mouse CD8$^+$ T cells (4). NKG2D recognizes several MHC-related ligands, including the UL16-binding protein and MHC class I-related chain family of proteins in humans (5, 6) and H60, RAE-1, and MULT-1 in mice (7–10). These NKG2D ligands, though usually absent from or expressed at low levels by normal adult tissues, are often induced on stressed, infected, or tumor cells in adult life (reviewed in Ref. 11). In this fashion, leukocytes expressing NKG2D can directly recognize transformed or infected cells.

Activation through NKG2D can have multiple outcomes including the production of IFN-γ and the triggering of cell-mediated cytotoxicity (5, 12). In αβ TCR$^+$ T cells, NKG2D has been suggested to provide a costimulatory role similar to CD28, enhancing TCR-mediated signaling events (13, 14). In vivo NKG2D is involved in antitumor as well as antiviral immunity (reviewed in Ref. 15).

NKG2D itself lacks intrinsic signaling capabilities. Like the TCR, NKG2D contains a positively charged amino acid within its TM region and requires association with adapter signaling proteins for cell surface expression. These adapter proteins contain complementary negatively charged amino acids within their TM regions that provide a salt bridge with NKG2D. Both in mice and humans, NKG2D homodimers associate with and signal through homodimers of the TM adapter protein DAP10 (12, 16). Signaling through DAP10 involves phosphorylation of its cytoplasmic YXXM motif, recruitment of the p85 subunit of phosphatidylinositol-3 kinase, and downstream signaling through AKT (16–18).

In mice, alternative mRNA splicing generates two functionally distinct isoforms of the NKG2D protein (12). The mouse NKG2D long (mNKG2D-L) protein comprises 232 amino acids, whereas the mouse NKG2D short (mNKG2D-S) protein lacks the first 13 N-terminal amino acids and initiates translation at a second methionine in the cytoplasmic domain of this type II protein. This shorter isoform is expressed in activated, but not resting, mouse NK cells and is capable of pairing with homodimers of either DAP10 or DAP12, an ITAM-containing TM adapter protein. Like other ITAM sequences, DAP12 intracellular $YXXL_{6-8X}$ YXXL/I motif recruits Syk family kinases (19). Mouse NKG2D-L pairs exclusively with DAP10 (12). Both DAP10 and DAP12 signaling contribute to NK cell-mediated cytotoxicity, whereas DAP12 signaling also definitively stimulates cytokine production, such as IFN-γ (12, 16, 20, 21).

The ability of the mouse NKG2D to generate identical receptors with distinct signaling properties by virtue of association with different adapter proteins prompted the question of whether human NKG2D also demonstrates this property. In this study, we have examined NKG2D expression and functional activity in human PBMCs of patients lacking a functional *DAP12* gene and have explored the structural basis for association of human and mouse NKG2D with the DAP10 and DAP12 adapter proteins.

Materials and Methods

Characterization of patients with Nasu-Hakola

The *DAP12* (*tyrobp*) gene in a patient with Nasu-Hakola, designated NH1, has a single base mutation in the start codon of exon 1 that has recently been identified in Japanese patients (22). Patients NH2 and NH3 have a single base deletion in exon 3 (22, 23). Loss of DAP12 protein expression in these patients was confirmed by Western blotting as previously described (22). Studies of all these subjects were conducted according to the institutional guideline.

Cytotoxicity assays

PBMC were prepared from peripheral blood samples of healthy individuals and three patients with Nasu-Hakola disease using density gradient centrifugation by using Ficoll-Hypaque Plus (Amersham Pharmacia Biotech, Uppsala, Sweden). PBMC were resuspended at 2×10^6/ml in RPMI 1640

*Department of Microbiology and Immunology and the Cancer Research Institute, University of California, San Francisco, CA 94143; and †Department of Immunology, National Institute of Neuroscience, National Center of Neurology and Psychiatry, Kodaira, Tokyo

Received for publication February 10, 2004. Accepted for publication June 7, 2004.

The costs of publication of this article were defrayed in part by the payment of page charges. This article must therefore be hereby marked *advertisement* in accordance with 18 U.S.C. Section 1734 solely to indicate this fact.

[1] This work was supported by The Irvington Institute for Immunological Research (to J.A.H.) and by National Institutes of Health Grant CA89189. L.L.L. is an American Cancer Society Research Professor.

[2] Current address: Center for Neurologic Diseases, Brigham and Women's Hospital, Harvard Medical School, 77 Avenue Louis Pasteur, Neuroscience Research Building Room 641, Boston, MA 02115-5817.

[3] Address correspondence and reprint requests to Dr. Lewis L. Lanier, Department of Microbiology and Immunology, University of California, 513 Parnassus Avenue, Health Sciences East Room 1001C, Box 0414, San Francisco, CA 94143-0414. E-mail address: lanier@itsa.ucsf.edu

[4] Abbreviations used in this paper: TM, transmembrane; EC, extracellular; mTM hEC, mouse-human NKG2D chimeras; IRES, internal ribosomal entry site; mCJS, murine cytoplasmic juxtamembrane sequence.

0022-1767/04/$02.00

medium supplemented with 10% FCS, 2 mM L-glutamine, HEPES, penicillin/streptomycin, and 2-ME. PBMC were plated into 24-well plates in the presence of 100 U/ml rIL-2, for mAb-induced redirected cytolytic assays, or 1000 U/ml rIL-2, for BaF/3 cytotoxicity assays rIL-2 (Shionogi, Osaka, Japan). A lower concentration of IL-2 was used for assays with P815 target cells as high doses of IL-2 cause considerable background cytotoxicity against P815, likely due to lymphokine-activated killer activity. Activated PBMC were harvested after 48-h culture, then used in 4-h ^{51}Cr release cytotoxicity assays as described (24). BaF/3, BaF/3 cells expressing MICA*0019, and FcR$^+$ P815 cells were labeled with 100 μCi of ^{51}Cr (PerkinElmer, Boston, MA) for 2 h at 37°C, washed three times, and used as target cells in cell-mediated cytotoxicity assays. For mAb-induced redirected cytotoxicity assays using P815 target cells, PBMC were cultured in the presence of medium only, control mAb anti-CD56 mAb (Leu19; BD Immunocytometry Systems, San Jose, CA) or anti-NKG2D mAb (made in collaboration with Dr. J. Houchins; R&D Systems, Minneapolis, MN). Monoclonal Abs were used at a final concentration of 2.5 μg/ml.

cDNAs, chimeras, and plasmids

Human "short" NKG2D, human truncated NKG2D, mouse truncated NKG2D, mouse-human NKG2D chimeras (mTM hEC), and NKG2D-CD69 chimeras were created by standard PCR mutagenesis. TM regions were determined by using the following TM prediction programs and a consensus sequence was obtained by comparison of the analyses: Tmap (http://srs.ebi.ac.uk/srsbin/cgi-bin/wgetz?-page+Launch+-id+1dvsK1MjgHZ+-appl+tmap+-launchFrom+top); DAS (http://www.sbc.su.se/~miklos/DAS/); Tmpred (http://www.ch.embnet.org/software/TMPRED_form.html); HMMTOP (http://www.enzim.hu/hmmtop/html/submit.html); SOSUI (http://sosui.proteome.bio.tuat.ac.jp/cgi-bin/sosui.cgi?/sosui_submit.html); and TMHMM (http://www.cbs.dtu.dk/services/TMHMM/). Protein chimeras and truncations were created using the following amino acids: mΔNKG2D begins at K48, hΔNKG2D at R47, and ΔCD69 at V39 (with numbering beginning at the first amino acid in the mNKG2D-L isoform and the human NKG2D and CD69 sequences). Mouse NKG2D TM construct consists of amino acids K48-V84 and the human NKG2D TM constructs span R47-N80. Human NKG2D extracellular (EC) construct begins at L82, and the human CD69 EC construct at G65. The human NKG2D short intracellular region construct consists of M15-E48, the human long intracellular construct of M1-E48 and the mouse NKG2D tail construct spans M1-E13. CD69 cDNA was synthesized from mRNA isolated from Jurkat T cells stimulated 24 h with 25 ng/ml PMA (Calbiochem, Darmstadt, Germany) by reverse transcription with Superscript II (Invitrogen Life Technologies, Carlsbad, CA). Site-directed mutagenesis was performed using a Quick Change kit (Invitrogen Life Technologies), according to the manufacturer's instructions. All constructs were confirmed by DNA sequencing. cDNAs were subcloned into pMx-pie (containing a puromycin resistance gene, an internal ribosomal entry site (IRES) element, and the enhanced GFP gene) or pMX-puro retroviral vectors (25).

Cells and transfectants

Plasmid constructs were transfected with Lipofectamine 2000 (Invitrogen Life Technologies) into the Phoenix packaging cell lines (generous gifts from Dr. G. Nolan, Stanford University, Palo Alto, CA) (26) to produce retroviruses. Retroviruses in medium containing 8 μg/ml polybrene (Sigma-Aldrich, St. Louis, MO) were used to infect BaF/3 reporter cells. Briefly, polybrene was added to retroviral supernatants and the mixture was used to resuspend BaF/3 reporter cells. Following centrifugation of the cells in the retrovirus-containing medium (1300 × *g* for 2.5 h), transfected reporter cells were incubated for 48 h at 37°C and then assayed for transgene expression. BaF/3 reporter cells were created from the mouse pro-B BaF/3 cell line. Dr. S. Tangye (Centenary Institute, Sydney, Australia) generously provided BaF/3 cells transfected with a mouse IL-3 cDNA to permit autocrine production of this requisite growth factor. To create Myc-DAP10 reporter cells, IL-3$^+$ BaF/3 cells were infected with retroviruses (pMX-puro vector) containing a cDNA including the human CD8 leader segment, followed by the Myc epitope (EQKLISEEDL) joined to the EC N-terminal domain of human DAP10 (27). Similarly, to create Flag-DAP12 reporter cells, IL-3$^+$ BaF/3 cells were infected with retroviruses (pMX-puro vector) containing cDNA including the human CD8 leader segment, followed by the Flag epitope (DYKDDDDK) joined to the EC N-terminal domain of human DAP12, as described (19, 28). Infected cells were then selected in RPMI 1640 medium supplemented with 10% FCS, 2 mM L-glutamine, and 1 μg/ml puromycin.

Flow cytometry and Abs

For immunofluorescence analysis of transfected *myc*-DAP10 BaF/3 reporter cells, 1 × 10^6 cells were stained with anti-*myc* mAb 9E11 (generously provided by Dr. G. Evan, University of California, San Francisco, CA), followed by a donkey anti-mouse IgG secondary Ab conjugated to PE (Jackson ImmunoResearch Laboratories, West Grove, PA). Cells were then preincubated in 10% normal mouse serum before being stained with either biotin-conjugated mouse anti-human NKG2D mAb (clone 149810, R&D Systems), biotin-conjugated rat anti-mouse NKG2D mAb CX5, or allophycocyanin-conjugated mouse anti-human CD69 mAb Leu23 (BD Pharmingen, San Diego, CA). Biotin-conjugated Abs were detected with CyChrome-conjugated or allophycocyanin-conjugated streptavidin (BD Pharmingen). For immunofluorescence analysis of transfected Flag-DAP12 BaF/3 reporter cells, 1 × 10^6 cells were stained with biotin-conjugated anti-Flag mAb M2 (Sigma-Aldrich), followed by CyChrome-conjugated streptavidin (BD Pharmingen). Cells were also stained prior with PE-conjugated mAb to mouse NKG2D (CX5), anti-human NKG2D, or anti-CD69 (Leu23; BD Pharmingen) followed by donkey anti-mouse IgG PE. Live cells were gated based on forward and side scatter profiles. Retrovirus-infected cells were gated based on GFP fluorescence. Cells were analyzed by using a FACSCaliber (BD Biosciences, San Jose, CA) or a small desktop Guava Personal Cytometer with Guava ViaCount and Guava Express software (Hayward, CA).

Immunoprecipitations and Western blots

A total of 50 × 10^6 transfected BaF/3 cells were solubilized in 1 ml Brij-Nonidet P-40 lysis buffer (0.875% Brij 97, 0.125% Nonidet P-40, 10 mM Tris base, 150 mM NaCl (pH 8.0), and protease inhibitors; all Sigma-Aldrich). Cell lysates were precleared with 60 μl of protein G-Sepharose beads (Amersham Pharmacia Biotech) for 1 h at 4°C. Anti-human NKG2D (clone 149810; R&D Systems) or isotype-matched control mAb were cross-linked to protein G beads by incubation in PBS for 30 min, followed by incubation in 10 mM dimethyl pimelimidate dihydrochloride (DMP; Pierce, Rockford, IL), 200 mM triethanolamine (Sigma-Aldrich) pH 8.2 for 45 min and extensive washing. Monoclonal Ab-coated beads were used for immunoprecipitation of precleared lysates for 3 h at 4°C. After washing, immunoprecipitates were eluted by adding nonreducing sample buffer and incubating for 30 min at room temperature. 2-ME (Sigma-Aldrich) was added, samples were boiled, and analyzed by 15% SDS-PAGE. Samples were transferred to Immobilon P membrane (Millipore, Bedford, MA), blocked and probed with goat anti-human DAP10 Ab N-17 (Santa Cruz Biotechnology, Santa Cruz, CA) or anti-human DAP12 mAb DX37 (27), followed by HRP-conjugated donkey anti-goat IgG (Amersham Pharmacia Biotech) or goat anti-mouse IgG (Amersham Pharmacia Biotech), respectively, and visualized with chemiluminescent substrate (Pierce).

Results

PBMCs from DAP12$^{-/-}$ patients display normal NKG2D function

Only the counterpart of the mNKG2D-L isoform has been described in humans and has been shown to coimmunoprecipitate with DAP10, but not DAP12 (16, 27). Nonetheless, this does not exclude a weak or indirect association between human NKG2D and DAP12 that may contribute to NKG2D receptor function in human lymphocytes. Therefore, studies were undertaken to address formally a potential role for DAP12 in human NKG2D receptor-dependent NK cell activation. Nasu-Hakola disease, also called polycystic lipomembranous osteodysplasia with sclerosing leukoencephalopathy, is a globally distributed recessively inherited disease caused by loss of function mutations in the *DAP12* (also called *tyrobp*) gene (23). In this report, we analyzed PBMC of three Japanese patients with Nasu-Hakola disease for their NKG2D-mediated cytolytic function. Each of these patients has a single point mutation in their *DAP12* gene that causes premature stop codons and results in a complete lack of detectable DAP12 protein (see *Materials and Methods*). We examined the peripheral blood CD3$^-$CD56$^+$ NK cells of these patients and found that the expression of NKG2D on the cell surface of their NK cells was indistinguishable from normal, healthy individuals (Fig. 1*a*). Previously, we reported that loss of function mutations in human *DAP12* did not affect expression of the closely linked *DAP10* gene (23); however, in this prior study NKG2D receptor-dependent functions were not directly analyzed.

To formally address the activity of the NKG2D receptor in patients lacking DAP12, we tested the ability of PBMCs from these

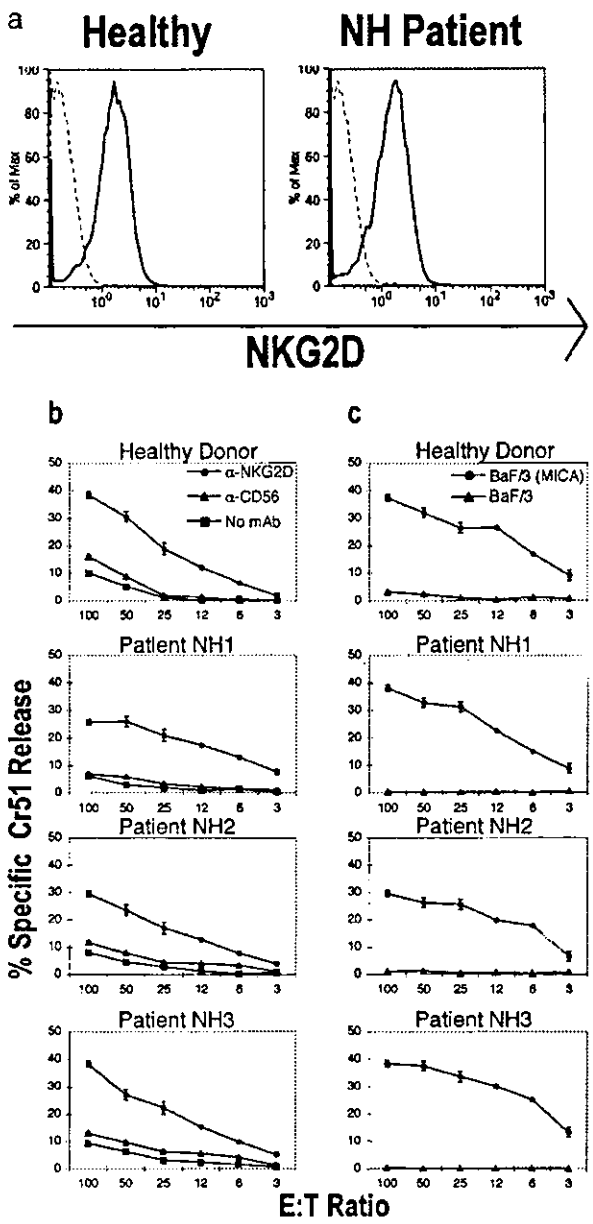

FIGURE 1. NKG2D expression and function in Nasu-Hakola patients. *a*, NKG2D levels on NK cells are identical in normal healthy humans and patients with Nasu-Hakola disease. $CD3^-CD56^+$ NK cells from PBMC of a normal, healthy individual, and Nasu-Hakola patients (NH1, NH2, and NH3) were stained with mAb against CD3, CD56, and NKG2D or appropriate control Ig and were analyzed by flow cytometry. Representative data from one Nasu-Hakola patient are shown. Isotype-matched Ig control (dashed line) and anti-NKG2D (bold lines) are shown. *b*, PBMC from a normal, healthy individual and three Nasu-Hakola patients (NH1, NH2, and NH3) were cultured for 48 h in IL-2 and assayed for mAb-induced redirected cytotoxicity against FcR^+ P815 target cells in the absence or presence of anti-NKG2D mAb or anti-CD56 mAb (used as a negative control). *c*, IL-2-activated PBMC from a normal, healthy individual, and three Nasu-Hakola patients (NH1, NH2, and NH3) were assayed for cytolytic activity against mouse Ba/F3 target cells or Ba/F3 cells stably transfected with MICA*0019, a human NKG2D ligand.

patients to kill target cells by the NKG2D-dependent pathway. This was achieved by using an anti-NKG2D mAb-induced redirected cytotoxicity assay and by using mouse target cells transfected with a human NKG2D ligand, MICA*0019. PBMCs from the three patients with Nasu-Hakola disease, as well as a normal, healthy individual, were cultured for 48 h in IL-2 and then used as effector cells in these cytotoxicity assays. Using ^{51}Cr-labeled FcR^+ P815 target cells, anti-NKG2D mAb induced cytotoxicity mediated by PBMCs of healthy individuals and patients with Nasu-Hakola disease, whereas the anti-CD56 mAb used as a negative control failed to augment lytic activity (Fig. 1*b*). No significant difference was seen in NKG2D-mediated cytotoxicity levels between the patient and control cells. To further characterize NKG2D function in patients with Nasu-Hakola disease, we performed cytotoxicity assays against BaF/3 mouse pro-B cells stably transfected with MICA*0019, a physiological ligand of human NKG2D. Although minimal cytotoxicity was seen against untransfected, parental BaF/3 cells, BaF/3 cells stably expressing MICA stimulated elevated cytotoxicity from activated PBMCs of both normal individuals and patients with Nasu-Hakola disease. No significant difference was observed in cytotoxicity levels mediated by PBMCs of healthy individuals and Nasu-Hakola patients against MICA-bearing target cells. Thus, NKG2D expression on NK cells and NKG2D-dependent functions were indistinguishable among healthy individuals and the patients with Nasu-Hakola disease. These experiments demonstrate normal human NKG2D function in the absence of DAP12.

Unlike mouse NKG2D-S, human NKG2D does not associate with DAP12

Many NK receptors, including NKG2D, KIR2DS, Ly49D, NKR-P1C, NKp30, NKp44, NKp46, and CD94/NKG2C, are multisubunit receptor complexes that convey signals via the TM adapters FcεRIγ, CD3ζ, DAP10, or DAP12 (reviewed in Ref. 29). All of these adapters have a negatively charged aspartic acid residue in their hydrophobic TM domain, which is critical for interaction with an oppositely charged basic residue in their associated ligand-binding receptors. For NKG2D, this basic residue is a conserved arginine in the TM region (Fig. 2*a*, starred residue). The human and mNKG2D-L receptors have been shown to pair and signal through DAP10, but not DAP12 (12, 16).

Recently, a second isoform of mouse NKG2D was discovered that lacks the first 13 N-terminal cytoplasmic amino acids and uses an alternative methionine start site due to alternative splicing of the transcript (12, 30). This shorter murine NKG2D isoform is capable of pairing and signaling with both DAP10 and DAP12 adapters (12, 30). Examination of the predicted amino acid sequence of human NKG2D reveals that it also contains a second N-terminal methionine residue that could potentially act as an alternative start site (Fig. 2*a*). Although to date no alternatively spliced human transcript involving the NKG2D cytoplasmic domain has been identified (31), it is impossible to exclude the existence of such isoforms at a low abundance or that they are only expressed in certain conditions of activation or in selected cell types. Therefore, we have addressed the issue using a different approach. In this model, we ask whether a theoretical short human NKG2D isoform lacking the first 14 amino acids could be able to pair with DAP12.

To address this experimentally, we artificially created a short human NKG2D using the second methionine residue as the start site and tested its ability to pair with DAP10 and DAP12. For these assays, we used mouse BaF/3 reporter cells stably transfected with Myc epitope-tagged human DAP10 or with Flag epitope-tagged human DAP12. In the absence of an associated receptor, Myc-DAP10 and FLAG-DAP12 were expressed at only low levels on the cell surface of the reporter cells. These reporter cells were infected with retroviruses encoding the wild-type human NKG2D (in our study designated as hNKG2D-L), the artificially created

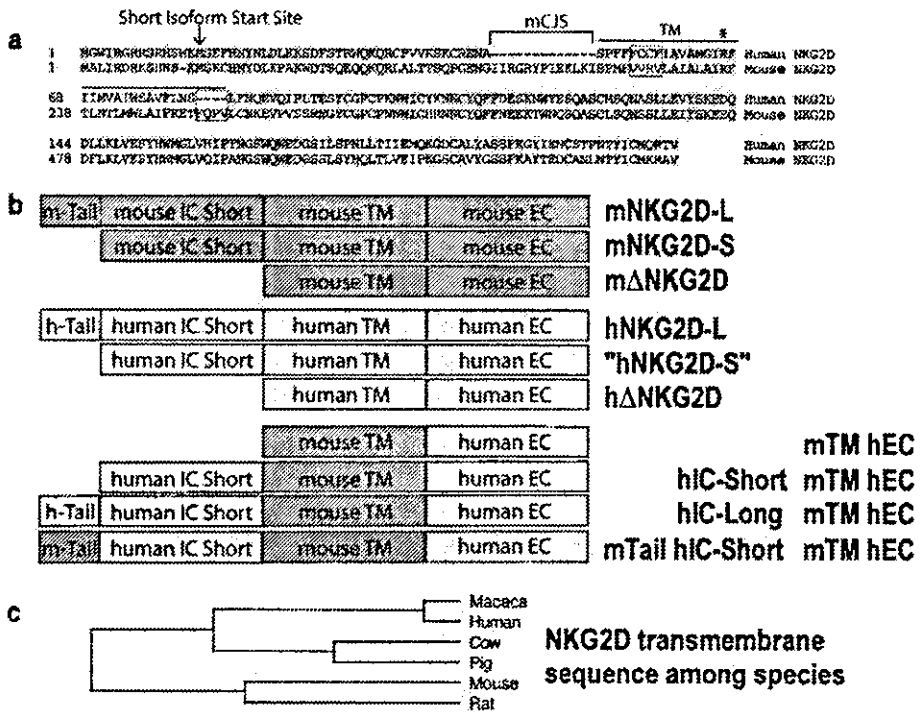

FIGURE 2. Human and mouse NKG2D comparisons and receptor constructs. *a*, Alignment of predicted mouse and human NKG2D amino acid sequences. Identical residues (shaded) in the mouse and human proteins are shown. An arrow indicates the methionine (M) beginning of the mouse NKG2D-short isoform and the artificial human "NKG2D-Short" protein. The mCJS (brackets) present in mouse, but not human, NKG2D is shown. The putative TM region (overlined) is starred to indicate the conserved arginine (R) residue required for association with DAP10 (16). Putative TM regions were defined as the consensus from six TM prediction programs (see *Materials and Methods*). Regions and residues (boxed) of interest are shown. *b*, Schematic representation is shown of the truncations and chimeric proteins generated, with the boundaries as defined in *Materials and Methods*. *c*, Phylogenetic comparison of the TM regions of NKG2D in the indicated species, as determined by Clustal W analysis of the proteins using MegAlign (DNASTAR Software, Madison, WI).

human "short" NKG2D (or hNKG2D-S), mNKG2D-L, and mNKG2D-S or an empty retroviral vector. The pMX-pie retroviral vector used in these experiments harbors an IRES-GFP element downstream of the inserted cDNA, allowing for infected cells to be readily detected by the expression of green fluorescence.

Cells were stained with mAbs against the appropriate epitope tags and either human or mouse NKG2D. Infected cells, detected by gating on GFP-positive cells using flow cytometry, were then analyzed for coexpression of NKG2D and the epitope-tagged adapter protein of interest. Coordinate expression of NKG2D and its associated adapter protein on the surface of transfected cells is indicated by the "diagonal" relationship observed in the bivariate dot plots. The long NKG2D proteins of both species and the mNKG2D-S protein paired with DAP10, as would be expected

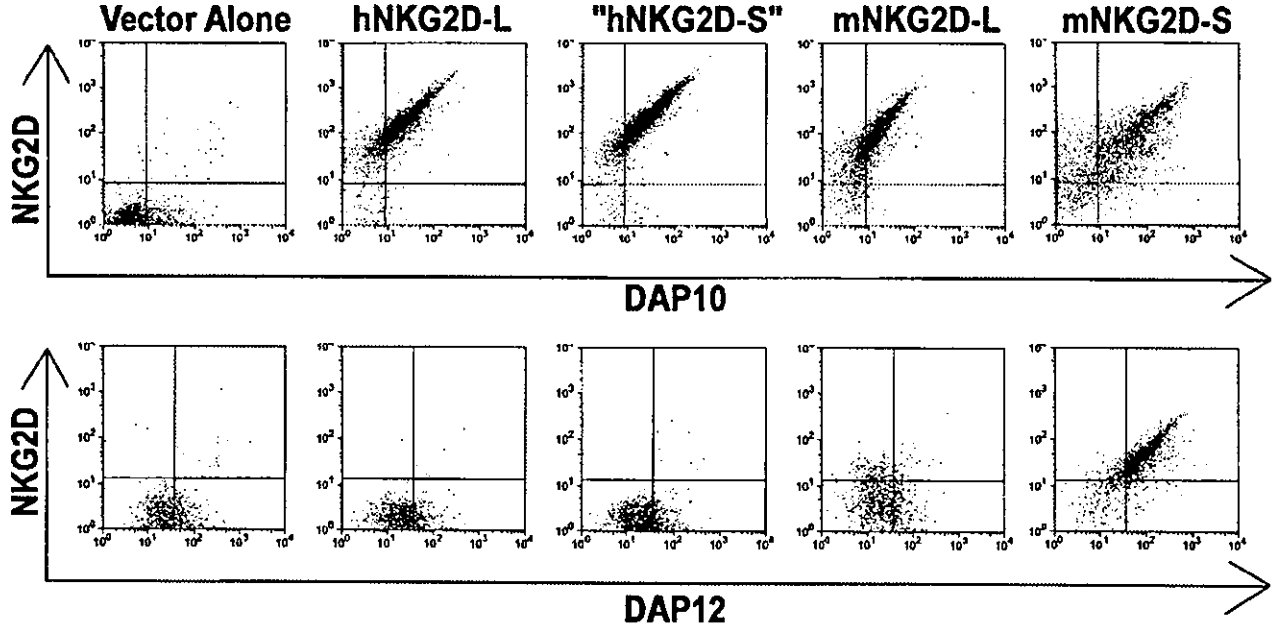

FIGURE 3. Unlike mNKG2D-S, human short NKG2D does not pair with DAP12. Ba/F3 reporter cells stably expressing Myc-DAP10 (*upper panels*) or Flag-DAP12 (*lower panels*) were infected with retroviruses with the indicated NKG2D constructs in a vector containing an IRES-GFP element. Samples were stained with the relevant anti-NKG2D and anti-epitope tag mAbs and analyzed by flow cytometry. Data shown are gated on GFP$^+$ cells, which confirmed expression of the construct in the infected cells. Results shown are representative of at least three independent experiments.